

Neuroprotective Effects of N-Acetyl Cysteine in an Acute Model of LPS Induced Neuroinflammation

By

JUDI KESEBI

A Dissertation Submitted to the
Graduate School of Health Sciences
in Partial Fulfillment of the Requirements for
the Degree of
Master of Science
In
(Neuroscience)



**KOÇ
ÜNİVERSİTESİ**

Date

Neuroprotective Effects of N-Acetyl Cysteine in an Acute Model of LPS Induced Neuroinflammation

Koç University

Graduate School of Health Sciences

This is to certify that I have examined this copy of a master's thesis by

Judi Kesebi

and have found that it is complete and satisfactory in all respects,
and that any and all revisions required by the final
examining committee have been made.

Committee Members:

Prof./ Assoc. Prof / Assist. Prof. ABC (Advisor)

Prof./ Assoc. Prof / Assist. Prof. ABC (Advisor)

Prof./ Assoc. Prof / Assist. Prof. ABC (Advisor)

Date: _____

To my loving parents,
for your endless love and support



“This Study was conducted using the service and infrastructure of Koç University
Research Center for Translational Medicine (KUTTAM)”



Neuroprotective Effects of N-Acetyl Cysteine in an Acute Model of LPS Induced Neuroinflammation

Judi Kesebi

Master of Science in (Neuroscience)

Month Day, Year

Abstract:

Neuroinflammation has been a major focus for researchers in the fields of neurology and neuropathologies, as it had proven to play a key role in triggering pathogenesis of various neurodegenerative diseases like Alzheimer's disease, where inflammation, among many other interconnected factors including oxidative stress and mitochondrial dysfunction plays a crucial role in the pathological feedback loop contributing to disease progression. Therefore, there is an inevitable need for implicating variable models of neuroinflammation, and it remains promising to investigate potential therapeutics, those with a natural origin in particular. LPS induced neuroinflammation is a widely used model in animal research, and is able to mimic intrinsic neuroinflammatory states seen in the human CNS by activating microglia and initiating the release of several proinflammatory cytokines. Numerous studies have pointed out the relevance of glial cells, like astrocytes and microglia to neuroinflammation, thus to possibly linked protein abnormalities like Tau fibrillary tangles and amyloid plaques. Moreover, recent works are focusing on the microglial activation derived perineuronal net disruptions in neurodegenerative and neuropsychiatric disorders. These disruptions might hold the answer to understanding the vulnerability of particular neuronal types to neuroinflammation.

In this project, we investigated the neuroprotective role of N-Acetylcystein, a well-known natural antioxidant, on an acute, 10 day model of centrally injected LPS rats. Animal Groups consisted of healthy controls, LPS-induced animals, NAC treated LPS-induced and a group treated with an additional prophylactic dose of NAC prior to model induction. We assessed the anti-inflammatory potential of NAC in terms of neuronal loss, perineuronal net degradation, glial cell activation, and protein aggregations, in addition to cognitive decline, using immunofluorescence stainings, ELISA and a behavioral test for working memory. Our results indicated that NAC was able to reduce LPS-induced A β ₁₋₄₂ accumulations in the brain and spinal cord, as well as to halt neuronal loss and inflammatory astrocytosis in variable regions of the hippocampus. Moreover, NAC administration clearly protected PNN structures and alleviated PNN density loss associated with LPS-induced microglial activation in the prefrontal cortex. These results indicate the potential neuroprotective and anti-inflammatory impact of NAC on early neuroinflammation-associated CNS pathologies, and highlights the need

for more in-depth investigation regarding the neuro-protective role of NAC in models of inflammatory neurodegeneration.



ACKNOWLEDGEMENTS

Hereby, I would like to thank my beloved supervisor, Prof.Dr Yasemin Gürsoy Özdemir for her constant motivation and guidance, having the kindest heart to fit a world yet the finest mind to create, develop, and convey knowledge in the best way possible. Words fail to describe my gratitude for your invaluable patience.

Dear Esra, you are an exceptional person that I will always be glad I met. Thank you for being a true mentor on many levels, thank you for giving me your time when I knew you needed it for yourself.

I further would like to thank my lab mates, without whom nothing would have been the same. Narges, my go-to person, loving sister, kind advisor, and organizer, thank you for raising me up each time I fell along the way. Ceyda, I am so thankful that we shared a path along this road, you gave me the best company and made me smile even when days were tough. Thank you for your pure heart, you deserve all the best.

Selin, Fatmanur, Dr.Pelin, thank you for being the colleagues anyone wishes for, doing science with you has been fulfilling!

I am deeply indebted to my support system, my mother and father and my lovely sisters, none of what I have become would have been possible without you believing in me, your love and your continuous support.

Finally, to my loving husband, thank you for making this easier than it could have been, for your patience, your support, for giving me perspective on many levels. I love doing life with you.

Article I. Table of Contents

Chapter 1:	1
INTRODUCTION	1
1.1. Neuroinflammation in Neurodegenerative Disorders	1
1.2. Oxidative Stress and Its Link to Neuroinflammation	1
1.3. Oxidative Stress in Alzheimer’s Disease	2
1.4. The Use of LPS in Models of Neuroinflammation	2
1.5. Defining Dementia	3
1.5.1 Alzheimer’s Disease.....	4
1.5.1.1 AD Hallmarks	4
1.6. N-Acetylcysteine	5
1.7. Perineuronal Nets	5
1.8. Perineuronal Net Disruptions in Neuroinflammatory States	6
1.9. N-Acetyl Cysteine and Perineuronal net Disruptions	7
Chapter 2:	8
MATERIALS AND METHODS	8
2.1. Animals	8
2.2. Study Groups and Experimental Design	8
2.3. Surgery and Model Induction	11
2.4. Behavioral Assessment	12
2.5. NAC administration	13
2.6. Animal Sacrifice and Tissue Collection	14
On the day of sacrifice, all animals were deeply anesthetized with ketamine/xylazine cocktail given intraperitoneally (0.1 mL/100g) combined with isoflurane gas.	14
2.7. Immunofluorescence Staining of Frozen Sections	14
2.8. Image Analysis	17
2.9. ELISA	17

2.10 Statistical Analysis	18
Chapter 3:	19
RESULTS:	19
3.1. ELISA Results:	19
3.1.1. A Single Intrahippocampal LPS Dose (10 µg) Increased Aβ Concentration in Brain and Spinal Cord Homogenates.....	19
ELISA results were statistically analysed through GraphPad Prism using Kruskal Wallis test for over all comprison (p=0.0026 for brain samples and p=0.004 for spinal cord samples) and Mann-Whitney U test for pairwise comparisons (p values indicated in Figure 5). Results indicated that Aβ ₁₋₄₂ concentration was significantly increased in brain homogenates of G2 (LPS injected rats), as well as in spinal cord homogenates when compared to controls (p<0.05) (Figure 5)	19
3.1.2. N-Acetylcysteine Significantly Reduced Aβ ₁₋₄₂ Concentrations to Control Levels	19
3.1.3. No Pronounced Difference in pMAPT/pTAU Concentration Between Groups	20
3.2. Behavioral Results: Administered Dose of LPS (10 µg) and/or Model Duration Did Not Cause Significant Memory Loss or Cognitive Dysfunction.	21
3.3. NAC Prevented LPS Induced Neuronal Loss in Hippocampal Regions	22
3.4. NAC Administration Reduced LPS Induced Astrogliosis	24
3.5. NAC Reversed PNN Loss Induced by LPS Injection in the Prefrontal Cortex	27
Chapter 4:	32
DISCUSSION	32
Chapter 5	36
CONCLUSION	36
Bibliography	37
Table 1 Experimental Groups	9
Table 2 Antibodies used for IF staining.....	17
Figure 1 Experimental Timeline.....	10
Figure 2 Weight change for all groups throughout the experiment.....	11
Figure 3 Image of animals post-operation.....	12
Figure 4 Apparatus used as MWM.....	13

Figure 5 Tissue preparation for freezing.....	16
Figure 6 A β 1–42 ELISA Results. Kruskal Wallis results indicated an overall significant difference between groups (p=0.0026). Quantification of A β 1–42 concentration in brain and spinal cord homogenates revealed a significant increase in A β 1–42 levels in brain homogenates in G2 compared to controls (Mann Whitney U results: p=0.0079). NAC clearly prevented the increase in A β 1–42 concentration by keeping levels close to controls (Mann Whitney U results: G3 vs control p=0.0714, G4 vs control p=0.0714). Similar results were seen in spinal cord samples, where Kruskal Wallis results indicated an overall significant difference (p= 0.0004). Moreover, according to Mann Whitney U results, G2 homogenates displayed significantly higher levels of A β 1–42 than controls (p=0.0357). No significant difference in A β 1–42 concentrations between G3 and G4 for both brain and spinal cord homogenates (p= 0.400 and p=0.3333 respectively).	20
Figure 7 pTAU ELISA Results. Quantification of Tau concentration in brain and spinal cord homogenates revealed an increasing trend in LPS applied groups but it did not reach to significance (p=0.3333). Although prophylactic and non-prophylactic application of NAC show decreased trend it has no significance.....	21
Figure 8 MWM Results. Latency in seconds taken by animals to reach the platform. Upon recording the time in seconds taken by animals of each group to reach the platform, results analysed using Kruskal Wallis test showed no significant difference between groups, indicating no potential cognitive/memory loss induced by LPS (p=0.9842 for Day3) and (p=0.2675).	22
Figure 9 Neuronal Count in Hippocampal Regions. (Only significant differences are indicated). Neuron cellular count in hippocampal regions in LPS-induced group was significantly reduced when compared to controls (Mann Whitney U: p=0.0417). Prophylactic application of NAC in G4 clearly protected neuronal loss and kept neuronal counts significantly higher than LPS-induced animals (Mann Whitney U: p=0.0340) and close to controls (Mann Whitney U: p=0.8477).....	23
Figure 10 Representative images of brain hippocampal sections. Hippocampal sections stained for neurons by a special neuronal marker (NeuN in red) and DAPI (in blue). Upper two images are for stained sections of the LPS-induced group (G2) and lower two are from controls (G1), regions are shown in two different magnifications.....	24
Figure 11 Analysis Results of GFAP Stainings Measures of GFAP integrated density (left) indicated an overall significant difference tested by Kruskal Wallis (p<0.0001). Mann Whitney U test results demonstrated a significant increase in GFAP intDen compared to controls (p<0.0001). NAC treated groups (G3 and G4) significantly reduced GFAP intDen when compared to G2 (p<0.0001 for both comparisons). Kruskal Wallis results for overall group comparisons for GFAP+ %area (right) indicated a significant difference between groups (p>0.0001). Mann-Whitney U results indicated an increase in GFAP stained %area in LPS group compared to controls (p<0.0001). G3 and G4 groups showed a significant reduction in GFAP expression when compared to LPS group (p<0.0001 for both).	25
Figure 12 Representative images of GFAP stained brain sections. GFAP stained brain slices showing the third ventricle (Red: GFAP, Blue: DAPI). Animals in G2 group received a single intrahippocampal dose of LPS (10 μ g) in total to both hippocampi, there is a clear reactivity in astrocytes featured by increased GFAP expression. Animals in G2 group were treated with NAC (i.p. 200 mg/kg) for 10 days post LPS-injection. Compared to LPS-injected group, there is a clear reduction in GFAP reactivity in NAC treated brains.....	26
Figure 13 Representative images of GFAP stained hippocampal regions (red: GFAP, Blue: DAPI). Animals the LPS group received a single intrahippocampal dose of LPS	

(10µg) in total to both hippocampi, there is a clear increase in GFAP expression compared to controls. Animals in NAC-treated group were i.p injected with NAC (200 mg/kg) for 10 days post LPS-injection. Prophylactic-NAC treated animals recieved an additional NAC injection prior to model induction. Compared to LPS-injected group, GFAP reactivity in NAC treated and prophylactic NAC treated brains is significantly reduced..... 27

Figure 14 Quantification of PNN surrounded neurons in the PFC. Kruskal Wallis test indicated an overall significant difference between all groups ($p<0,0001$). Average count of WFA (PNN marker) surrounded neurons in the PFC of LPS-injected animals were significantly lower than controls ($p<0,0001$). Average number of WFA surrounded cells in NAC treated animals (G3) and prophylaxis group (G4) was significantly higher when compared to LPS-injected group ($p<0,0001$)..... 28

Figure 15 Loss of PNNs in LPS induced animals. On the left, IF stained brain slice of the PFC from a control animal (NeuN in red indicating neurons, WFA in green staining PNN structures and DAPI in blue). On the right: same staining applied on a brain slice of the PFC from an LPS-injected animal. Images depict a prominent loss of WFA+ neuronal surroundings in LPS-injected animals compared to controls. 29

Figure 16 WFA stained PFCs in all groups. PNN surrounded neurons (white arrows). Red: NeuN, Blue: DAPI, Green: WFA. Staining against PNNs with WFA revealed a significant loss in PNN structures in regions of the PFC in LPS-induced animals. Stained brain slices from prophylactic NAC treated and NAC treated groups indicated that NAC provided some preservation of PNN structures against LPS. 30

Figure 17 WFA stained PFCs in all groups. (Blue: DAPI, Green: WFA). Staining against PNNs with WFA revealed a significant loss in PNN structures in regions of the PFC in LPS-induced animals. Stained brain slices from prophylactic NAC treated and NAC treated groups indicated that NAC provided some preservation of PNN structures against LPS. 31



ABBREVIATIONS

CNS = Central Nervous System

AD = Alzheimer's Disease

NAC = N-Acetylcysteine

LPS = Lipopolysaccharide

PNN = Perineuronal Nets

IF = Immunofluorescence

WFA = Wisteria floribunda agglutinin

Cy3 = Cyanine

MWM = Morris Water Maze

DAPI = 4',6-diamidino-2-phenylindole

DPBS = Dulbecco's Phosphate Buffered Saline

ECM = Extracellular Matrix

i.p = Intraperitoneal

OCT = Optimal Cutting Temperature Compound

PFA = Paraformaldehyde

MAPK = Mitogen-Activated Protein Kinase

NF- κ B = Nuclear factor kappa-light-chain-enhancer of activated B cells

DAMP = Damage-Associated Molecular Patterns

ROS = Reactive Oxygen Species

RNS = Reactive Nitrogen Species

GABA = γ -Aminobutyric acid



Chapter1: INTRODUCTION

1.1. Neuroinflammation in Neurodegenerative Disorders

Neuroinflammation is an essential biological process in which multiple cell types such as microglia, astrocytes, neutrophils, monocytes and neurons play a role. (Hey-Kyeong Jeong, 2013). With highly complex features, controlled neuroinflammation governs brain homeostasis in cases of brain damage resulting from insults either of an endogenous origin or exogenous pathogens; however, if inflammation persists to chronic states it may lead to serious pathologies (Wang & Qi, 2022). Therefore, models of neuroinflammation are recently playing an essential role in unraveling the pathways behind inflammatory driven CNS pathologies linked to several neurodegenerative diseases like Alzheimer's disease (Nazem et al., 2015), Parkinson's disease (Troncoso-Escudero et al., 2018) and multiple sclerosis (Bjelobaba et al., 2017). Such models are also of a highly practical significance in screening for potential inflammatory drugs. The pathological cascade driven by neuroinflammation includes CNS associated hallmarks like microglial activation, astrogliosis and release of pro-inflammatory cytokines, as well as recruitment of peripheral immune cells which leads to blood-brain barrier damage and subsequent neuronal loss (More et al., 2013). Additionally, neuroinflammation is now considered as a significant associative to oxidative stress, one of the main drivers for several neurological disorders (Anwar, 2022).

1.2. Oxidative Stress and Its Link to Neuroinflammation

The brain is a highly susceptible organ to oxidative damage due to its high dependency on oxygen (utilizing about 20% of body's total oxygen usage). Moreover, the chemical nature of the brain is featured by a high content of lipid polyunsaturated fatty acids as well as high metal ion concentration, which indeed act as core inducers of oxidative stress (Anwar, 2022). The resulting imbalance between levels of ROS (reactive oxygen species) and antioxidants in the brain leads to serious brain tissue damage directly linked to the activation of TLR-4 (Toll-like receptor) inflammatory cascades (Sayre et al., 2001). Furthermore, an elevation in ROS was shown to activate disease associated

molecular patterns (DAMP), which in turn increases levels of NF- κ B and MAPK in glial cells, essentially in microglia and astrocytes, and exacerbates the inflammatory cascade (Anwar, 2022).

Importantly, such activation of microglial and astrocyte cells driven by DAMPs initiates several molecular events that facilitate abnormal protein accumulations like A β plaques and neurofibrillary TAU tangles, main hallmarks of Alzheimer's disease, leading eventually to apoptotic neuronal loss (Birecree et al., 1988) thus progressive cognitive decline and brain atrophy.

1.3. Oxidative Stress in Alzheimer's Disease

Recent clinical work has shown increased records of late onset AD among the elderly without previous predisposing factors or related genetic background (Anwar, 2022).

Oxidative stress and accumulating reactive oxygen species have been a major focus being a potential cause for late onset AD especially the neuroinflammatory type. It has been suggested that increased oxidative stress levels that results from either extrinsic or intrinsic sources leads to homeostatic disruptions linked to oxidative stress/antioxidant balance, this leads to a further accumulation of ROS and RNS in addition to proinflammatory molecules. Resulting chronic inflammation interferes with natural gene expression leading to protein misfolding, then eventually amyloid beta deposition and leading to neuronal loss and cognitive decline.

Overproduction of ROS in the central nervous system was shown to be associated with clinical features of AD, such as amyloid beta deposition (Wang, 2010), mitochondrial dysfunction, as well as increased intracellular Ca⁺² and associated excitotoxicity (Anwar, 2022). Furthermore, oxidative stress is shown to induce an overexpression of MAPK and NF κ B pathways both in astrocytes and microglia via the activation of DAMPs. This leads to the release of nitric oxide and other factors associated with Amyloid deposition and accumulation of Tau tangles (Anwar, 2022)

1.4. The Use of LPS in Models of Neuroinflammation

It is now known that in case of an insult, both innate and adaptive immune responses of the inflammatory type are seen in the CNS, through a cascade of cytokine and chemokine release and activation of microglia (Amor et al, 2010).

LPS injection in animals, either intracerebrally or via systemical way in variable doses, serves as a mimic for human AD by inducing the same key hallmarks, starting from oxidative stress (Sugaya K et al, 1998) and ending in cognitive decline (Lee et al, 2008). Lipopolysaccharide (LPS), is an endotoxin of a bacterial origin that is known to trigger inflammatory responses in rodents and thus has been used to induce models of neuroinflammation in a wide range of neurodegenerative disease studies (Batista CRA et al, 2019). For instance Lee and colleagues (2008) demonstrated that LPS induced neuroinflammation stimulates amyloidogenesis associated cognitive decline in mice. Moreover, LPS was shown to be able to activate glial cells and oxidative stress markers in rats (Sugaya K et al, 1998).

LPS causes the activation of TLR-4 found on the surface of microglia, and inhibiting the TLR-4 pathway prevents LPS induced neuroinflammation and associated cognitive decline (Zhao et al, 2019).

Furthermore, a study (Koedel et al, 2007) showed that mice lacking the TLR2 and TLR4 receptors displayed lower cytokine release and thus less pro-inflammatory reactions upon traumatic brain injury.

It was further shown that advanced glycation end products (AGE) are accumulated in AD, and their receptors (RAGE) are over-expressed on the surface of neurons and astrocytes. Such increase in these receptors is seen in oxidative stress and neuroinflammatory processes as well. Which suggests a role of RAGE's in the propagation of disease pathology (Amor et al, 2010).

1.5. Defining Dementia

Dementia is a clinical condition manifested by a range of symptoms related to cognitive dysfunction. It is defined as impaired cognitive ability that interferes with one's routine activities and executive functions, which significantly affects their quality of life.

Multiple cognitive domains are seen to be impaired in people with dementia, including memory, learning, spatial orientation, and mood (Arvanitakis et al, 2019).

Lately, with the increasing life span of the human population, dementia is rising as a major health problem with pronounced economic and social burden. It is now estimated that dementia sufferers are 47 million, with this number expected to reach 131 million by 2050 (Hebert et al, 2013).

While age stands as an important risk factor for dementia, it is also seen in younger population, and several other risk factors are highly attributed to early onset cognitive decline associated with dementia. These include genetics, hypertension, diabetes, diet, and poor exercise of social and physical activity (Pal et al, 2018) (Gupta et al, 2015) as well as head trauma (LoBue et al, 2019). Moreover, recent studies are focusing on the role that chronic neuroinflammation plays in increasing the risk of dementia, for instance Ahmad et al (2022) highlighted the link between persistent neuroinflammatory-induced microglial activation and dementia.

1.5.1 Alzheimer's Disease

Alzheimer's disease (AD) is the most common type of dementia accounting for about 75% of all dementia cases (Qiu, 2009). AD is a multifaceted neurodegenerative disease, characterized by progressive cognitive decline associated with pathological accumulation of misfolded proteins and a cascade of other pathological hallmarks leading to neuronal loss. Recently, AD has been imposing a huge burden on public health due to the increasing percentage of elderly population and the economic burden is huge as the cost of dementia in 2010 was reported to be approximately \$157 billion (Hurd et al, 2013). The field of AD studies is therefore particularly focused on attempting to unravel the key pathological events associated with this disease, as well as discover potential treatments.

1.5.1.1 AD Hallmarks

Key underlying mechanisms of AD pathology are considered to be neuroinflammation, oxidative stress, and hippocampal neurodegeneration. This is because they are thought to link other factors contributing to disease progression such as mitochondrial dysfunction and protein aggregation. Thus, it is essential to study the causal link between these mechanisms and the basic hallmarks of AD, as well as those of other neurodegenerative diseases. Katafuchi et al, (2012) and Krstic et al, (2012) demonstrated this causal link by showing that both oxidative stress and neuroinflammation induce AD associated amyloid pathology, a key hallmark of AD, through glial activation. Moreover, oxidative stress is shown to induce an overexpression of MAPK and NFkB pathways both in astrocytes and microglia via the activation of DAMPs.

This leads to the release of nitric oxide and other factors associated with Amyloid deposition and accumulation of Tau tangles (Anwar, 2022)

1.6. *N-Acetylcysteine*

N-acetylcysteine is a natural antioxidant of the thiol type with anti-inflammatory activity which acts through regulating the activation of NF- κ B and HIF-1 α , as well as directly scavenging reactive oxygen species (ROS) (Vida Mokhtari, 2017). The important role NAC plays as an antioxidant is through generating glutathione, one of the intrinsic antioxidants that have an essential role in redox regulations. Glutathione stands as an essential endogenous antioxidant, functioning in multiple roles associated with the regulation of immune responses (Shahripour et al, 2017) and regulating signal transduction through modulating oxidation-reduction reactions. During oxidative stress, NAC acts as a source of cysteine, one of the three amino acids that form the structure of glutathione and is the key limiting factor in GSH synthesis since it is the one less available intracellularly in normal conditions (Shahripour et al, 2017) (Aruoma, 1989). Various levels of evidence focus on the importance of NAC in restoring the body's antioxidant systems in chronic inflammation where there is an elevation in levels of ROS (Shahripour et al, 2017). For instance, Amin and colleagues (2008) indicated that NAC was able to reduce mitochondrial membrane depolarization. Similarly, in their review, Moreira et al, (2007) indicated the significant role of NAC in reducing oxidative and apoptotic markers resulting from mitochondrial damage in Alzheimer's disease patient fibroblasts. Furthermore, Fu Al et al (2006) showed that NAC administration was able to preserve learning and memory abilities in A β -induced AD mice models assessed by Morris water maze.

1.7. *Perineuronal Nets*

Perineuronal nets have recently been driving the attention in the field of neuropathology, with recent literature focusing on their role in neurodegenerative and neuropsychiatric disorders. PNNs which are highly specialized extracellular matrix structures that enwrap particular neurons, preferentially fast spiking parvalbumin-expressing (PV+) GABAergic inhibitory interneurons of the hippocampus and cerebral cortex (Wen et al, 2018). They form an essential part of the tetrapartite synapse and contribute majorly to signal transduction (C. Reichelt, 2019). Moreover, interactions between neurons and their surrounding perineuronal nets form the essence of synaptic plasticity. For instance, immunostainings of the adult rat visual cortex showed that perineuronal net maturation overlaps with the closure of the critical period of plasticity, a time window of highly dynamic synapse formation, and neuronal interconnections (Pizzorusso T et al, 2002). Indeed, perineuronal nets play an essential role in aiding neuronal maturation and differentiation (Ana Jakovljevic, 2021). Therefore, researchers have particularly focused on these structures as a potential method in the treatment of several neurodegenerative and neuropsychiatric diseases, such as dementia (A.Suttkus et al, 2016) and schizophrenia (A. Mauney et al, 2013).

1.8. Perineuronal Net Disruptions in Neuroinflammatory States

One of the key downstream consequences of chronic neuroinflammation and oxidative stress is the disruption of extracellular matrix structures, including perineuronal nets, that normally surround and protect neurons from neurotoxins and damaging factors, such as reactive oxygen species. For instance, C.Reichelt (2020) indicated that chronic microglial activation, a main hallmark of AD pathology, is responsible for increasing the burden of neuronal damage, mainly by disrupting perineuronal net components; as chronically activated microglia respond to cell damage by activating TLR4 (Anwar, 2022) and releasing proinflammatory cytokines, as well as particular proteinases that cleave these components, stripping away the protective shield around neurons (C.Reichelt, 2020). Having such a major protective role against oxidative stress, microglial induced degradation of PNN components, as seen in AD, can render neurons vulnerable to damage, resulting in a feedback loop inducing microglial activation, PNN degradation, amyloid aggregation and neuronal death (D. Crapser J et al, 2020). Interestingly, it is not only microglial cells that engulf damaged perineuronal nets. D. Crapser (2020) showed that inclusions of aggrecan, a major component of the

perineuronal net structure, were found in amyloid plaques in mice models of AD. These findings raise important questions regarding the impact of neuroinflammation on PNN structures and how this phenomenon translates in terms of cognitive dysfunction seen in AD thus contributes to disease progression.

1.9. N-Acetyl Cysteine and Perineuronal net Disruptions

Given what was mentioned above, saving perineuronal nets from structural damage seen in multiple neurodegenerative diseases can serve as a key factor to halt neuronal loss. One way to achieve that is to target oxidative stress as a way to maintain balanced Redox regulations thus save ECM loss. In their research paper, Sharmin S (2021) showed that when administered postnatally, NAC was able to prevent PNN destruction in a transgenic mouse model of intrinsic defective PNN structures. Similarly, it was indicated that NAC was able to prevent delayed maturation of parvalbumin expressing interneurons and their surrounding PNNs in a mouse model of redox dysregulation (Cabungcal et al, 2013). In both works, NAC was administered early during the post-natal and pubertal period, respectively, which is known to be a highly flexible window for PNN maturation. Importantly, after puberty, PNN structures come to a mature state with reduction in their dynamic abilities, making it difficult to manipulate them pharmaceutically for the aim of neuroprotection against inflammatory damages associated with oxidative stress.

The aim behind this project was to build upon those works by investigating the neuro-protective impact of NAC by focusing on the basis of neuronal loss, astrocytic activation, amyloidosis and perineuronal net disruptions, along with behavioral assessment of the cognitive dysfunction in adult rats. Utilizing an acute model of neuroinflammation, we conducted a comprehensive analysis on LPS induced neuroinflammation that mimics AD pathology. Moreover, we wanted to test the neuroprotective efficacy of N-acetylcysteine (NAC) on LPS induced inflammatory processes and underlying pathology seen in our model. Our major focus in this study was to test whether our LPS model of neuroinflammation could activate microglia enough to disrupt the structure of perineuronal nets thus stripping away the protective shield around neurons against oxidative stress. More importantly, this work may well be

the first to investigate the antioxidant role NAC plays to save PNNs in an acute model of neuroinflammation in adult animals.

Chapter 2:

MATERIALS AND METHODS

2.1. *Animals*

In house bred 46 adult male Wistar rats, 8-9 weeks of age, weighing 187g in average were used for the experiment.

Animals were allowed free access to standard laboratory rat chow and water, they were housed in standard cages maintained in temperature (20°C – 26°C), humidity (30% – 60%) and lighting (12 hours light/dark cycle) controlled room.

All experiments and procedures were carried out in the light phase (between 9.00 am. and 17.00. pm) in accordance with the protocols approved by the Institutional Animal Care and Use Committee (IACUC) at Koç University, and under compliance of the Animal Research Reporting In Vivo Experiments (ARRIVE) guidelines.

2.2. *Study Groups and Experimental Design*

Animals were randomly divided into 4 groups after assessing their motor function to exclude any abnormal motor deficits that might interfere with the results. Groups were then assigned as the following and shown in Table 1:

G1, Healthy control group (n=7): Rats were housed at the same conditions as other groups and underwent the same MWM trainings and MWM test.

G2, LPS only group (n=7): Rats received intrahippocampal LPS injections without any treatment.

G3, LPS+NAC group (n=7): Rats received intrahippocampal LPS injections followed by 4 separate NAC doses (200 mg/kg per dose), one dose every other day along 10 days.

G4, LPS+Prophylaxis group (n=7): Animals received a prophylactic NAC dose prior to LPS administration, in addition to 4 treatment doses after model induction (200 mg/Kg per dose), one dose every other day along 10 days.

As demonstrated in Figure 1, animals underwent habituation to the water maze where any potential intrinsic motor deficits were excluded. Following LPS administration, the model lasted for 10 days, during which animals underwent several MWM trainings, had regular weight measurements Figure 2 and (for groups G3 and G4) received intraperitoneal NAC injections (200 mg/kg) given every other day.

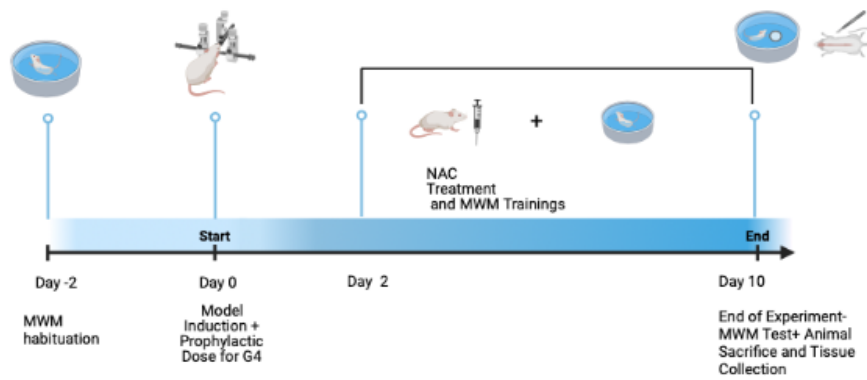
On the final day (10 days after model induction), MWM test was applied to assess the animals' retention of the platform, then they were sacrificed to collect tissues and samples.

Table 1 Experimental Groups.

Animal Group	Experimental Condition
G1	Healthy controls
G2	Rats received intra-hippocampal LPS injections (10 ul in total)
G3	Rats received intra-hippocampal LPS injections (10 ul in total) and received 4 separate NAC i.p. injections (200mg/kg per dose) after model induction along 10 days.
G4	Rats received a (200mg/kg) single dose of NAC prior to model induction,

underwent intra-hippocampal LPS injections (10 ul in total) and received 4 separate NAC i.p. injections (200mg/kg per dose) after model induction along 10 days.

Experiment Timeline



Created in BioRender.com bio

Figure 1 Experimental Timeline.

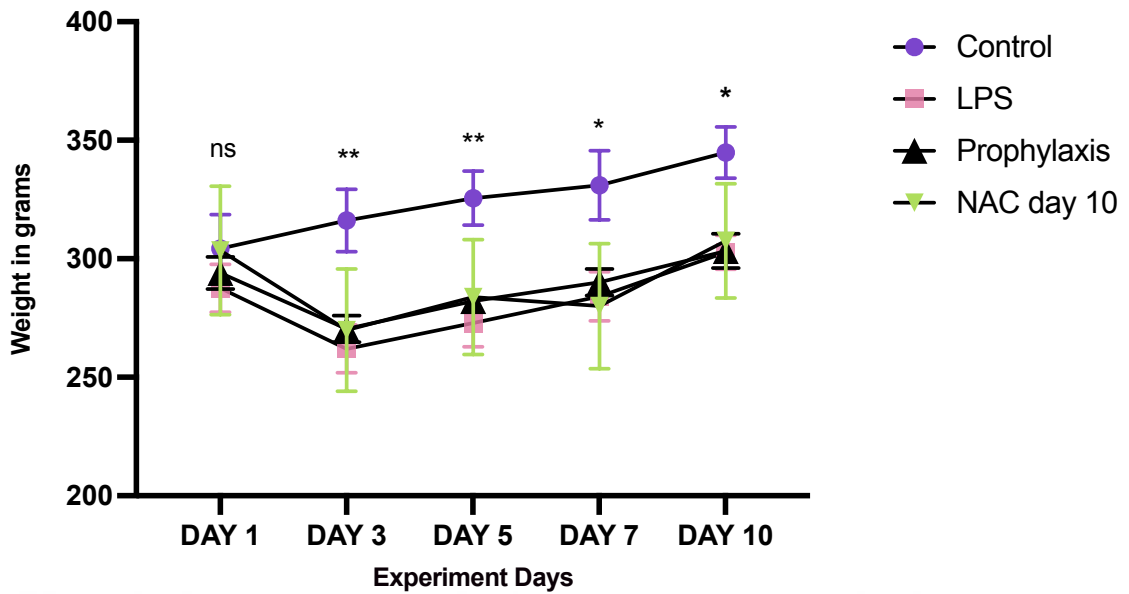


Figure 2 Weight change for all groups throughout the experiment.

2.3. Surgery and Model Induction

The model was induced by injecting LPS bilaterally into the rats' hippocampi, as LPS gram negative bacteria was proven to induce non genetically based neuroinflammatory type of AD (Catorce and Gevorkian, 2016). On the day of surgery, animals were anesthetized with ketamine/xylazine cocktail given intraperitoneally (0.1 mL/100g), then they were positioned on a rat specific stereotaxis apparatus (Stoelting, Wood Dale, IL, USA).

Lipopolysaccharide (LPS) purchased from Sigma, United States (Sigma-Aldrich, St. Louis, MO, L2630), was dissolved (1 mg/mL) in sterile PBS and 10 μ L in total were given to both hippocampi, injections were done with a micro-syringe through midsagittal holes drilled into the neocortex using the following coordinates: 3.6 mm anterior, 2 mm medial and 3.6 mm posterior, 2 mm lateral from the bregma, both at a depth of 3.4 mm. Coordinates chosen were in accordance with previous literature (Espinosa et al., 2013).

Surgical incisions were cleaned and closed with surgical staples Figure 3 , then animals were placed on a warming pad to maintain their body temperature until they recovered from anaesthesia.

Surgical procedure was done in accordance with rules and regulations of Institutional Animal Care and Use Committee (IACUC) at Koç University.



Figure 3 Image of animals post-operation.

2.4. Behavioral Assessment

In order to assess hippocampal memory, Morris water maze test was performed (Morris et al, 1982). Animals were handled by a single experimenter and in the same room during the whole procedure.

The apparatus used was a circular pool Figure 4 (152 cm diameter and 38 cm height), filled with clean tap water, the water temperature was maintained throughout the experiment ($26\pm 1^\circ$).

Platform used was transparent, 17 cm in length, hidden 2 cm below water and 20 cm from the pool wall in a fixed quadrant (the southwest quadrant).

On the first day, all rats were allowed to swim freely for 1 minute to get habituated to the pool and to exclude any preexisting motor weaknesses.

On the following day, the platform was hidden in the middle of the southwest quadrant, rats were then released into the water and allowed to swim until they found the

platform; rats that fail to locate the platform and escape within two minutes were gently guided to the platform and allowed to stand on it for 10 seconds, latency to find the platform was then recorded as 120 seconds.

On each training day, two trials were applied for each animal; starting from a different quadrant chosen randomly for each trial. Animals had a total of 4 training days and a final test day (10 days after LPS injections) to assess their learning and memory, and escape latencies were recorded for each animal throughout the experiment.

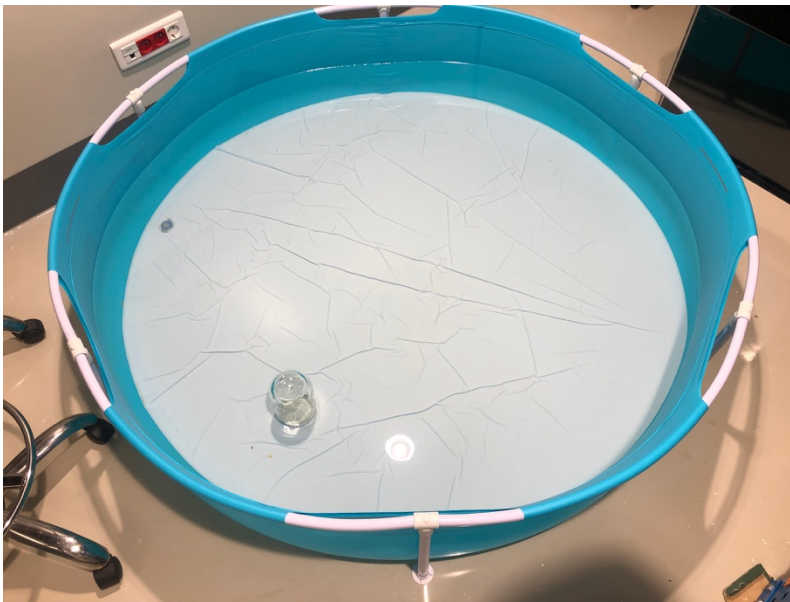


Figure 4 Apparatus used as MWM.

2.5. NAC administration

N-Acetyl Cysteine (NAC) was prepared from a pharmaceutically available mucolytic (ASIST, Bilimilac, Turkey) and dose was prepared with respect to NAC concentration. Each animal in G3 received one i.p. dose (200mg/kg) (Shahidi et al., 2017) of NAC starting from day 2 after surgery every other day until day 10. In addition to the same 4 doses, animals of the G4 group received one additional injection 4 hours prior to surgery and LPS induction to assess whether NAC has a prophylactic impact.

2.6. *Animal Sacrifice and Tissue Collection*

On the day of sacrifice, all animals were deeply anesthetized with ketamine/xylazine cocktail given intraperitoneally (0.1 mL/100g) combined with isoflurane gas.

Animals were divided randomly for immunohistochemical or protein analyses.

For histological studies, animals were transcardially perfused with 0,1M sterile phosphate buffer saline (PBS) followed by 4% PFA. Brains and spinal cords were removed and kept in 4% PFA overnight at +4°C.

For protein-based analyses, brains and spinal cords were removed without perfusion and homogenized with sterile PBS. Tissue homogenates were then kept at -80°C.

Cerebrospinal fluid samples were obtained and centrifuged at 15000g for 10 minutes at 4°C then stored at -80°C for subsequent analyses.

2.7. *Immunofluorescence Staining of Frozen Sections*

For histological analysis, collected brains and spinal cords were fixed with 4% PFA overnight at +4°C, then they were dehydrated with a sucrose gradient (10%, 20% and 30% respectively and 48 hours each). After that, frozen tissue blocks were prepared by embedding tissues in OCT (frozen tissue matrix) (OCT, Leica, #14020108926) and stored in -80°C Figure 5.

Tissue blocks were later sliced with a cryostat microtome (Leica CM 1850, Leica Microsystems, Seoul, Korea) at a thickness of 10 µm. To proceed with immunofluorescence staining, first, slides were washed with distilled water to melt OCT surrounding tissue slices, then they were incubated in methanol for 5 minutes to allow permeabilization and washed with Dulbecco's phosphate-buffered saline (DPBS, Gibco, #14190-094).

To prevent non-specific reactions, tissue slices were blocked using a commercially available blocking solution (Super Block, Thermo Fisher Scientific™, PI37535).

Following the blocking step, tissue slices were incubated with primary antibodies (diluted in Super Block) at 37°C for 1.5 hours. Excess non-bound primary antibodies were then washed with DPBS.

Subsequently, tissues were incubated with suitable secondary antibodies to allow the visualization of target proteins, followed by thorough washing steps with DPBS again. Lastly, slides were mounted with 4', 6-diamidino-2-phenylindole (DAPI, Abcam, Ab104139).

Antibodies used for immunostaining are summarized in Table 2.



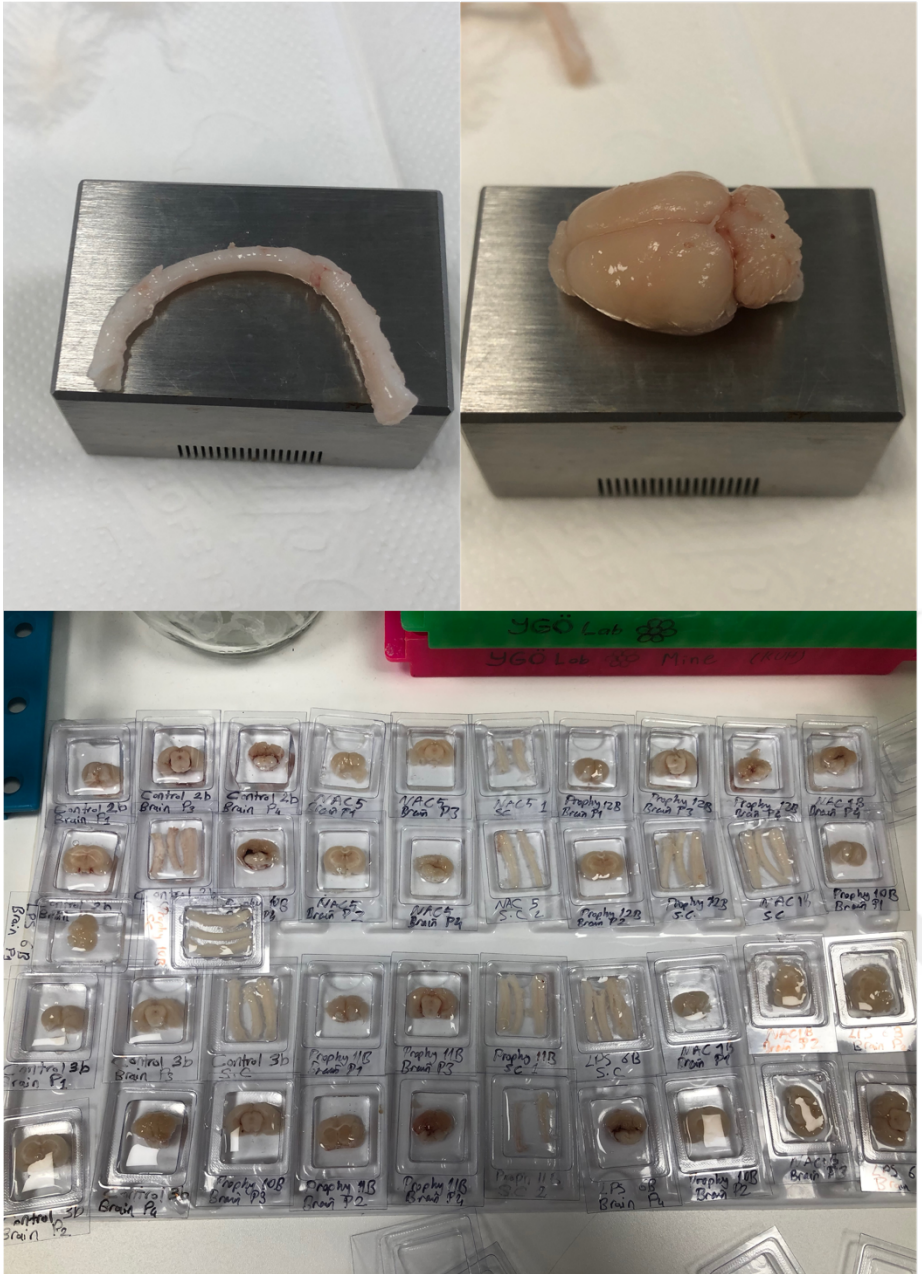


Figure 5 Tissue preparation for freezing.

Table 2 Antibodies used for IF staining.

Target	Primary Antibody (Catalog Number)	Dilution	Secondary Antibody	Dilution
Neurons	rabbit anti-NeuN (Abcam, Ab177487)	1/100	Goat-anti-rabbit Cy3	1/200
Astrocytes	rabbit anti-GFAP (Abcam, Ab7260)	1/100	Goat-anti-rabbit Cy3	1/200
Perineuronal Nets	WFA, Vector Labs, FL-1351-2)	1/500	Conjugated	

2.8. Image Analysis

Immunofluorescence stainings were observed using Leica DMI8 SP8 Confocal Scanning Microscope. Images from frozen sections were taken and exported as tiff files from the LAS X software (Leica, Wetzlar, Germany), then analyzed using ImageJ image processing program (NIH, MD, USA). For quantitative assessment of target markers, fluorescence intensities were compared between groups after collecting the images under the same applied microscopy settings, post-capture manipulations like contrast and background noise were also applied identically between groups. Differences between groups were analysed in matched areas and assessed for significance by One-way ANOVA or Kurskal Wallis tests using GraphPad PRISM (Version 9.2.0) (San Diego, USA).

2.9. ELISA

To assess inflammation induced pathology in terms of abnormal protein accumulation and in order to investigate the ability of NAC to reduce these hallmarks, commercially available ELISA kits (Elabscience, # E-EL-R3030 and # E-EL-R0943) were used to determine concentrations of Amyloid beta and Tau respectively in brain and spinal cord homogenates.

The protocol and sample preparation were applied in accordance with the manufacturer's instructions; target protein concentrations were determined compared with the standard curve.

ELISA results were compared between groups and differences were tested for significance using GraphPad PRISM (Version 9.2.0) (San Diego, USA).

2.10 Statistical Analysis

All results were expressed as mean \pm SD unless otherwise mentioned. GraphPad PRISM (Version 9.2.0) (San Diego, USA) was used for statistical analyses. Appropriate statistical test was used upon Shapiro Wilk normality test, respective One-way ANOVA or Kruskal Wallis tests were used for group comparisons to analyse differences in matched areas. A p-value less than 0.05 was considered statistically significant.

Chapter 3:

RESULTS

3.1. *ELISA Results:*

3.1.1. A Single Intrahippocampal LPS Dose (10 µg) Increased A β Concentration in Brain and Spinal Cord Homogenates.

ELISA results were statistically analysed through GraphPad Prism using Kruskal Wallis test for over all comprison ($p=0.0026$ for brain samples and $p=0.004$ for spinal cord samples) and Mann-Whitney U test for pairwise comparisons (p values indicated in Figure 6). Results indicated that A β_{1-42} concentration was significantly increased in brain homogenates of G2 (LPS injected rats), as well as in spinal cord homogenates when compared to controls ($p<0.05$) Figure 6.

3.1.2. N-Acetylcysteine Significantly Reduced A β_{1-42} Concentrations to Control Levels

In G3 (LPS+NAC) group, A β_{1-42} was significantly reduced when compared to G2 (LPS only group) in brain and spinal cord sample homogenates ($p<0.05$). Interestingly, G4 (LPS+prophylaxis) group showed more reduction than G3 in A β_{1-42} concentration when compared to LPS+NAC group and levels of A β_{1-42} were shown to be closer to controls, however, difference between G3 and G4 did not reach statistical significance ($p>0.05$) Figure 6.

These results indicate the need for further research on the prophylactic impact of NAC against amyloid pathology in models of neuroinflammation.

3.1.3. No Pronounced Difference in pMAPT/pTAU Concentration Between Groups

Our ELISA results represented in Figure 7 indicated no significant difference between groups in terms of pTAU concentration measured in brain and spinal cord homogenates ($p > 0.05$)

These results indicate that a single LPS dose (10 μg in total) given intrahippocampally or the duration of the model was not enough to initiate AD like pathology in terms of protein aggregation for 10 days. More importantly, these results prove that amyloid aggregation precedes tauopathy in this model of neuroinflammatory AD.

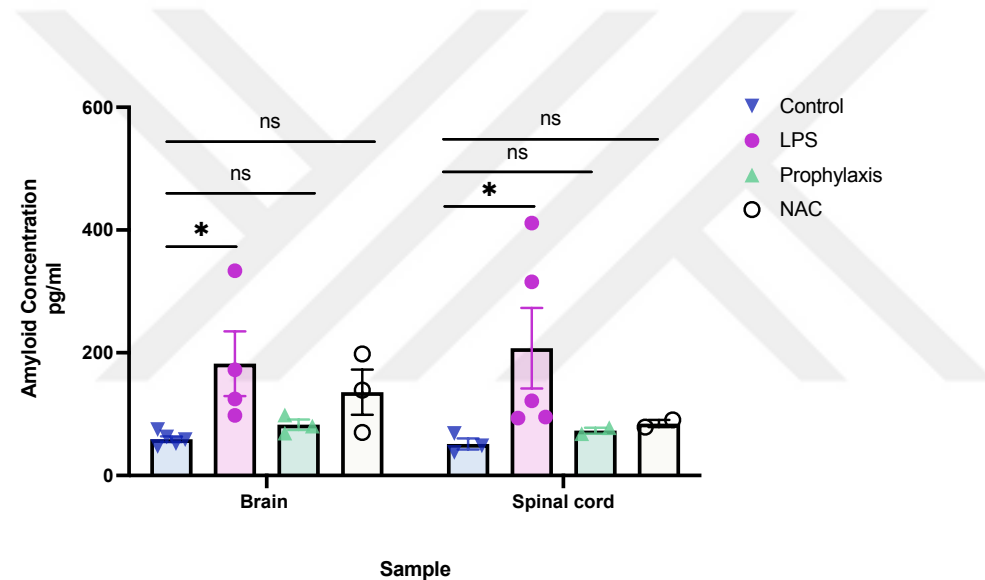


Figure 6 A β 1–42 ELISA Results.

Kruskal Wallis results indicated an overall significant difference between groups ($p = 0.0026$). Quantification of A β 1–42 concentration in brain and spinal cord homogenates revealed a significant increase in A β 1–42 levels in brain homogenates in G2 compared to controls (Mann Whitney U results: $p = 0.0079$). NAC clearly prevented the increase in A β 1–42 concentration by keeping levels close to controls (Mann Whitney U results: G3 vs control $p = 0.0714$, G4 vs control $p = 0.0714$). Similar results were seen in spinal cord samples, where Kruskal Wallis results indicated an overall significant difference ($p = 0.0004$). Moreover, according to Mann Whitney U results, G2 homogenates displayed significantly higher levels of A β 1–42 than controls ($p = 0.0357$).

No significant difference in A β 1–42 concentrations between G3 and G4 for both brain and spinal cord homogenates ($p= 0.400$ and $p=0.3333$ respectively).

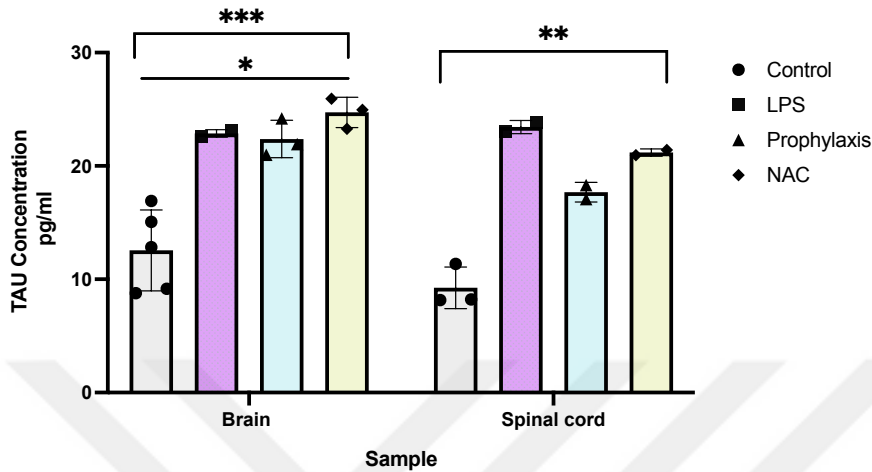


Figure 7 pTAU ELISA Results. Quantification of Tau concentration in brain and spinal cord homogenates revealed an increasing trend in LPS applied groups but it did not reach to significance ($p=0.3333$). Although prophylactic and non-prophylactic application of NAC show decreased trend it has no significance.

3.2. Behavioral Results: Administered Dose of LPS (10 μ g) and/or Model Duration Did Not Cause Significant Memory Loss or Cognitive Dysfunction.

Our MWM results indicate that there was no significant difference in terms of platform retention latencies between groups ($p>0.05$) (Figure 7). There is however a general decrease in time taken by all groups when comparing first (corresponding to day3 after LPS induction) and last test days indicating a learning pattern in all animal groups.

This result can be explained by saying that neuronal loss (as indicate in 3.3) and amyloid aggregation as seen in abovementioned results, precedes cognitive decline in this type of model and duration of the model was not sufficient to observe potential memory loss.

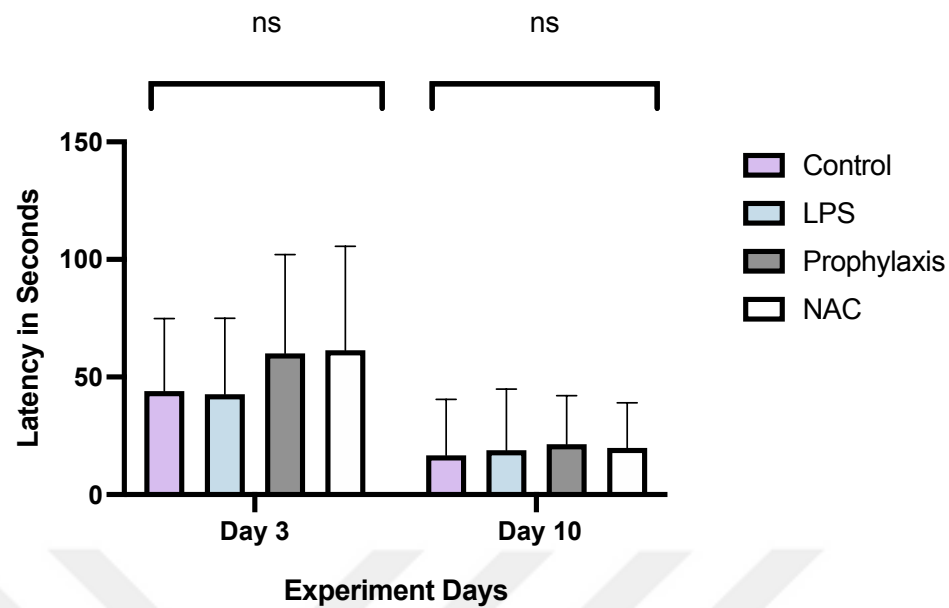


Figure 8 MWM Results. Latency in seconds taken by animals to reach the platform. Upon recording the time in seconds taken by animals of each group to reach the platform, results analysed using Kruskal Wallis test showed no significant difference between groups, indicating no potential cognitive/memory loss induced by LPS ($p=0.9842$ for Day3) and ($p=0.2675$).

3.3. NAC Prevented LPS Induced Neuronal Loss in Hippocampal Regions

To investigate whether the LPS dose administered, and duration of the model resulted in any significant neuronal loss, the number of NeuN positive cells was measured in different hippocampal regions (CA1, CA2, CA3 and DG) Figure 10 as well as in the parietal cortex using ImageJ software. Our results indicate that LPS induced a significant neuronal loss compared to control values ($p<0.05$). Moreover, Neuronal cell count measured in hippocampal regions of G4 (prophylactic NAC injection prior to model induction) was significantly higher when compared with G2 ($p<0.05$) Figure 9.

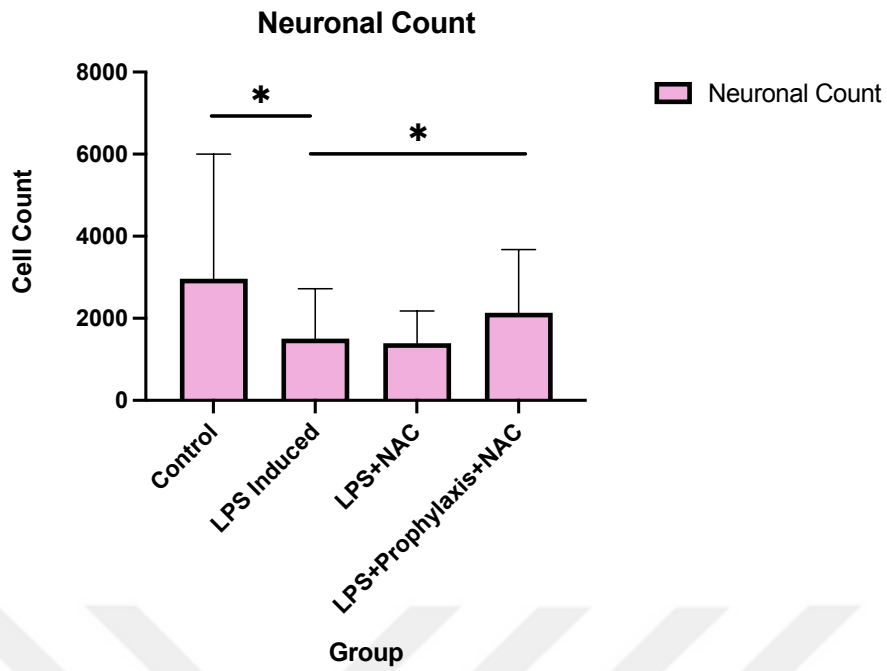


Figure 9 Neuronal Count in Hippocampal Regions. (Only significant differences are indicated). Neuron cellular count in hippocampal regions in LPS-induced group was significantly reduced when compared to controls (Mann Whitney U: $p=0.0417$). Prophylactic application of NAC in G4 clearly protected neuronal loss and kept neuronal counts significantly higher than LPS-induced animals (Mann Whitney U: $p=0.0340$) and close to controls (Mann Whitney U: $p=0.8477$).

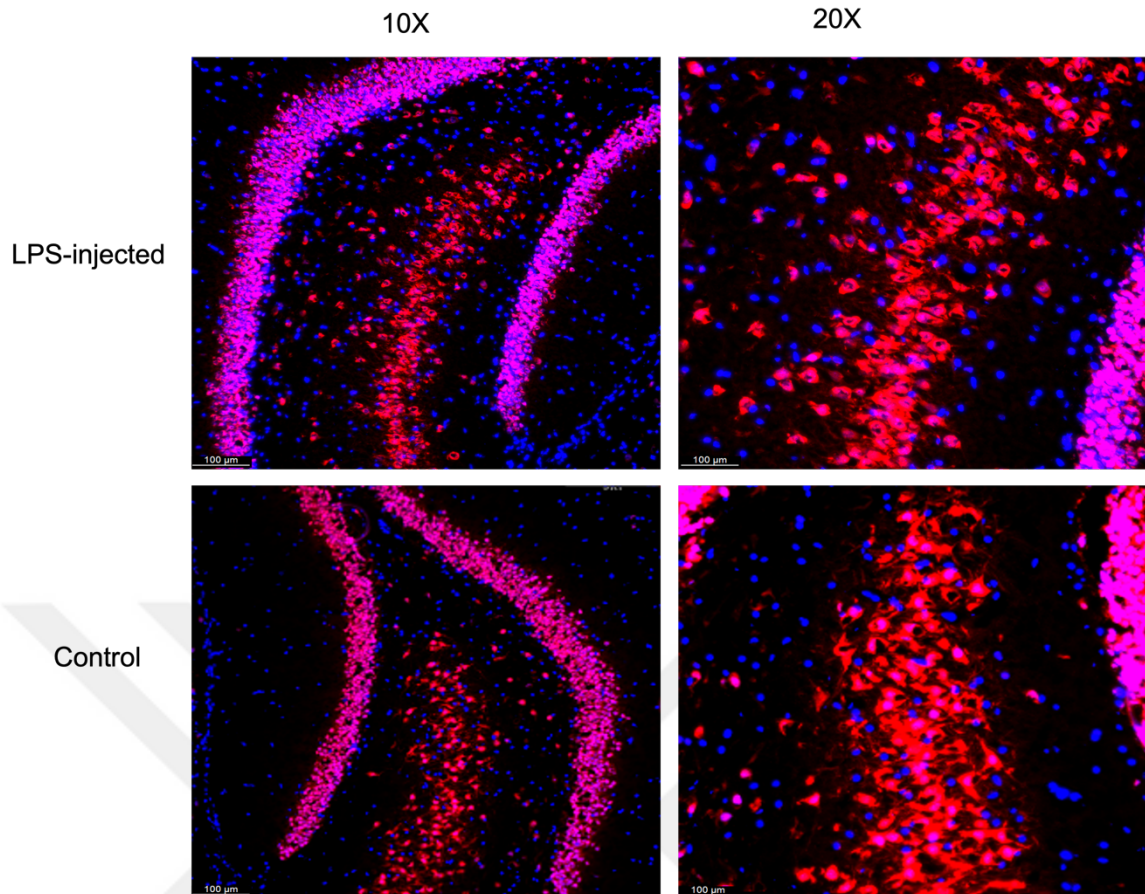


Figure 10 Representative images of brain hippocampal sections. Hippocampal sections stained for neurons by a special neuronal marker (NeuN in red) and DAPI (in blue). Upper two images are for stained sections of the LPS-induced group (G2) and lower two are from controls (G1), regions are shown in two different magnifications.

3.4. NAC Administration Reduced LPS Induced Astrogliosis

Upon measuring GFAP stained %area and integrated densities, results demonstrated a significant increase in astrocytic coverage corresponding to higher astrocyte count in hippocampal regions and parietal cortex in LPS induced animals compared to controls ($p < 0.05$). Moreover, when compared to LPS induced animals, animals in both G3 and G4 showed a significant reduction in GFAP stained area and integrated density ($p < 0.05$) Figure 11. This indicates that NAC administration reversed LPS induced astrogliosis Figure 12 Figure 13.

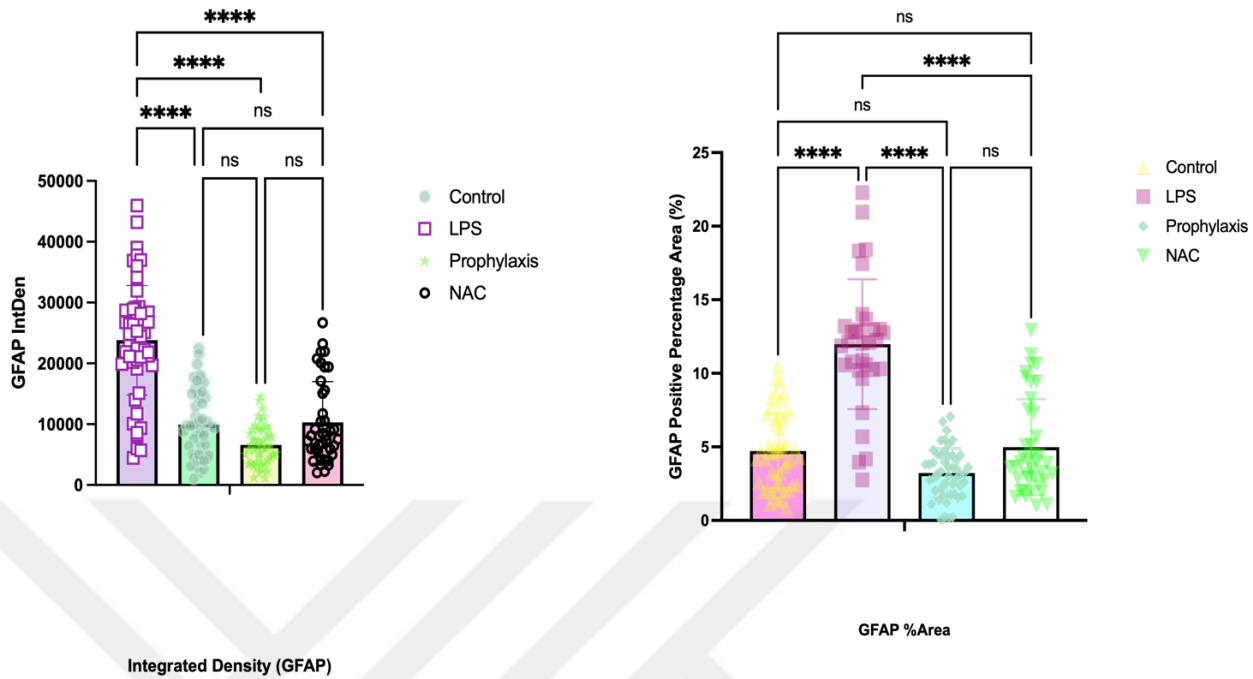


Figure 11 Analysis Results of GFAP Stainings Measures of GFAP integrated density (left) indicated an overall significant difference tested by Kruskal Wallis ($p < 0.0001$). Mann Whitney U test results demonstrated a significant increase in GFAP intDen compared to controls ($p < 0.0001$). NAC treated groups (G3 and G4) significantly reduced GFAP intDen when compared to G2 ($p < 0.0001$ for both comparisons). Kruskal Wallis results for overall group comparisons for GFAP+ %area (right) indicated a significant difference between groups ($p > 0.0001$). Mann-Whitney U results indicated an increase in GFAP stained %area in LPS group compared to controls ($p < 0.0001$). G3 and G4 groups showed a significant reduction in GFAP expression when compared to LPS group ($p < 0.0001$ for both).

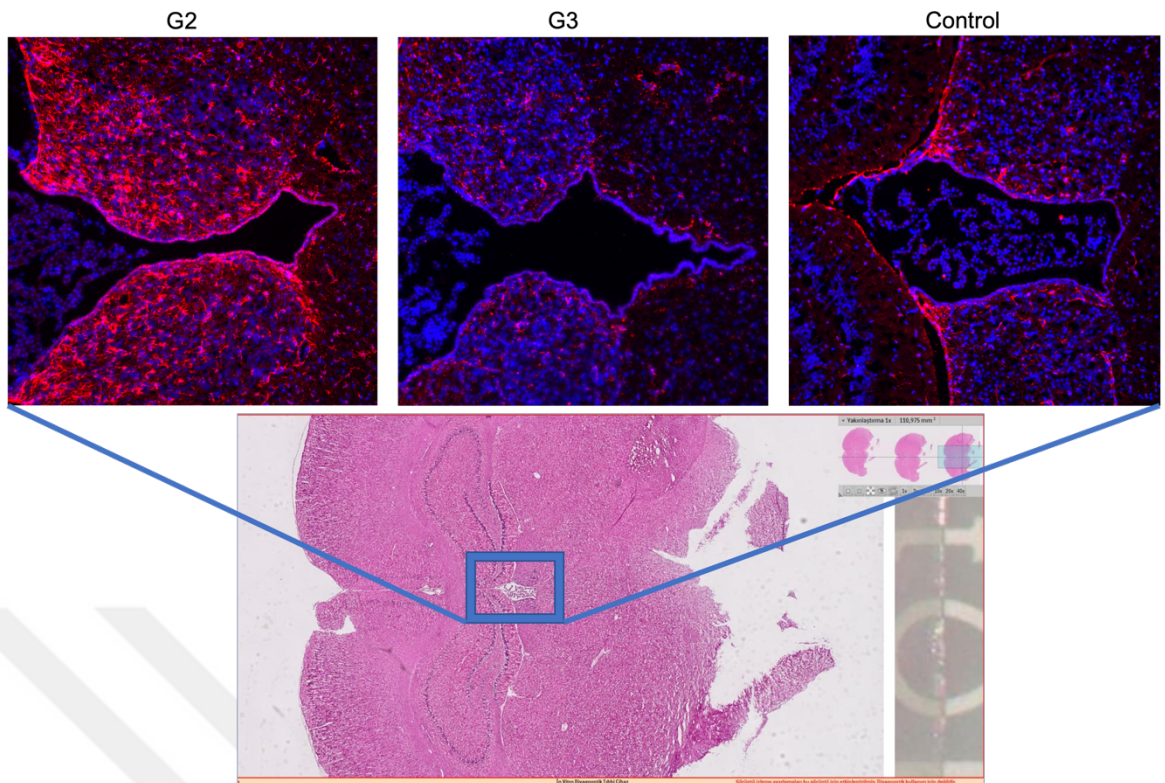


Figure 12 Representative images of GFAP stained brain sections. GFAP stained brain slices showing the third ventricle (Red: GFAP, Blue: DAPI). Animals in G2 group recieved a single intrahippocampal dose of LPS (10 μ g) in total to both hippocampi, there is a clear reactivity in astrocytes featured by increased GFAP expression. Animals in G2 group were treated with NAC (i.p. 200 mg/kg) for 10 days post LPS-injection. Compared to LPS-injected group, there is a clear reduction in GFAP reactivity in NAC treated brains.

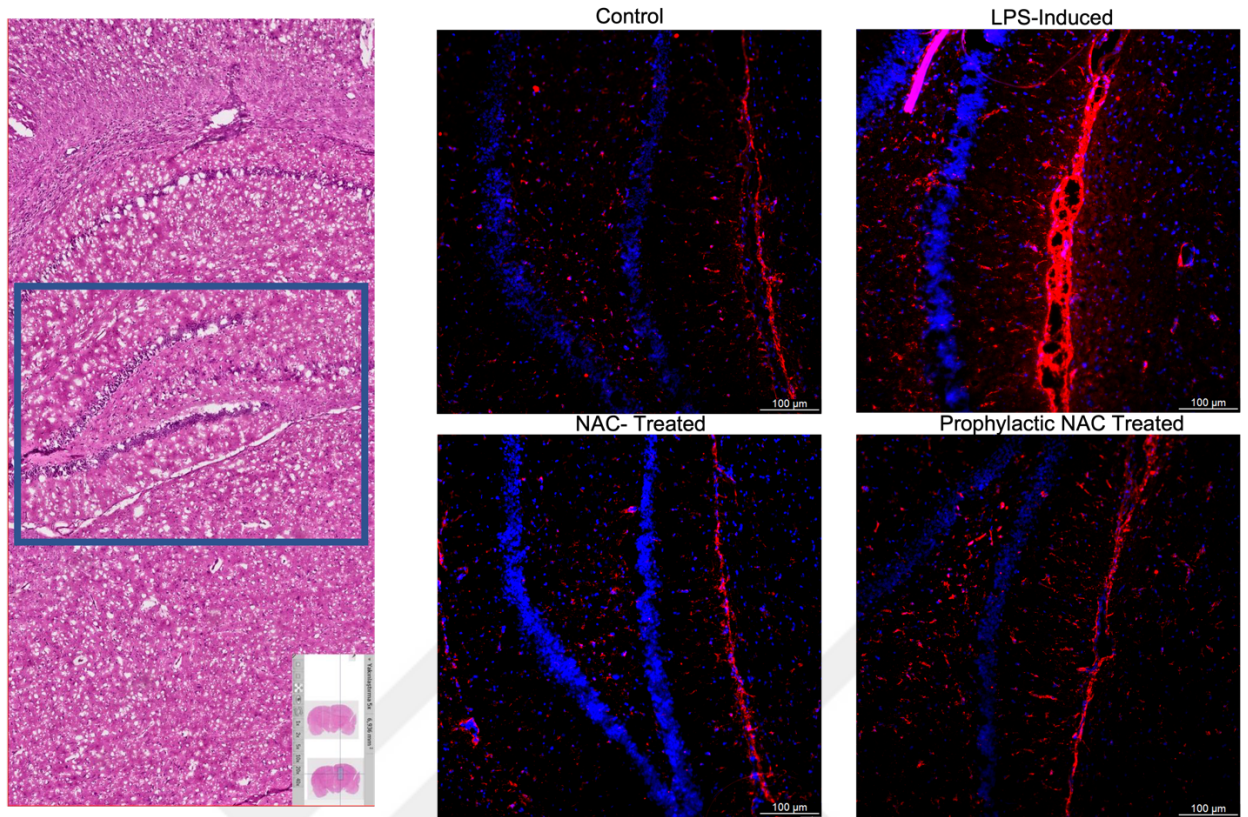


Figure 13 Representative images of GFAP stained hippocampal regions (red: GFAP, Blue: DAPI). Animals the LPS group received a single intrahippocampal dose of LPS (10µg) in total to both hippocampi, there is a clear increase in GFAP expression compared to controls. Animals in NAC-treated group were i.p injected with NAC (200 mg/kg) for 10 days post LPS-injection. Prophylactic-NAC treated animals received an additional NAC injection prior to model induction. Compared to LPS-injected group, GFAP reactivity in NAC treated and prophylactic NAC treated brains is significantly reduced.

3.5. NAC Reversed PNN Loss Induced by LPS Injection in the Prefrontal Cortex

Staining of perineuronal nets via the lectin WFA showed a pronounced decrease in the number of PNN surrounded neurons in the prefrontal cortex in LPS injected rats when compared to normal controls ($p < 0.05$) Figure 15. Results also demonstrate that in both LPS+NAC and LPS+Prophylaxis groups, the number of neurons

surrounded by WFA+ nets in the prefrontal cortex was significantly higher than LPS treated animals ($p < 0.05$) Figure 14, Figure 16.

This indicates a protective role of NAC against inflammatory LPS-induced perineuronal net loss in adult animals.

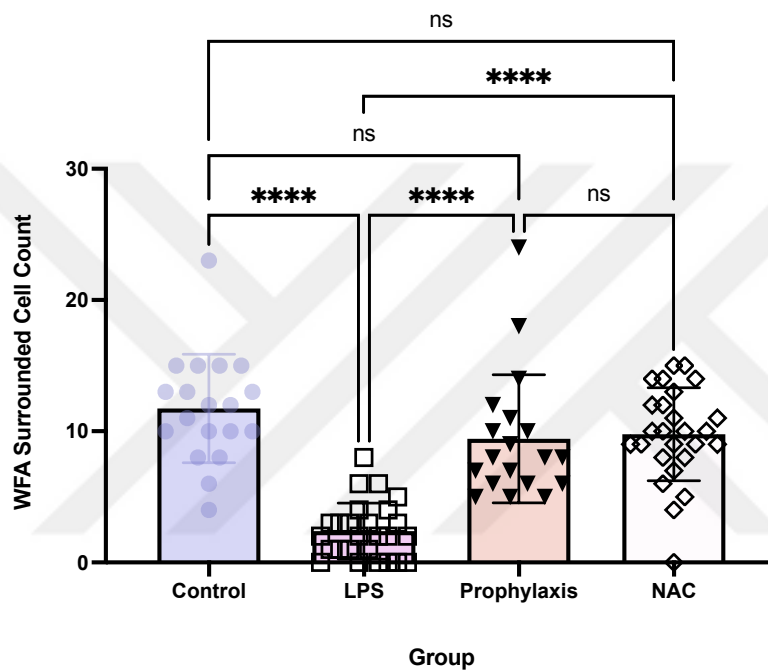


Figure 14 Quantification of PNN surrounded neurons in the PFC. Kruskal Wallis test indicated an overall significant difference between all groups ($p < 0,0001$). Average count of WFA (PNN marker) surrounded neurons in the PFC of LPS-injected animals were significantly lower than controls ($p < 0,0001$). Average number of WFA surrounded cells in NAC treated animals (G3) and prophylaxis group (G4) was significantly higher when compared to LPS-injected group ($p < 0,0001$).

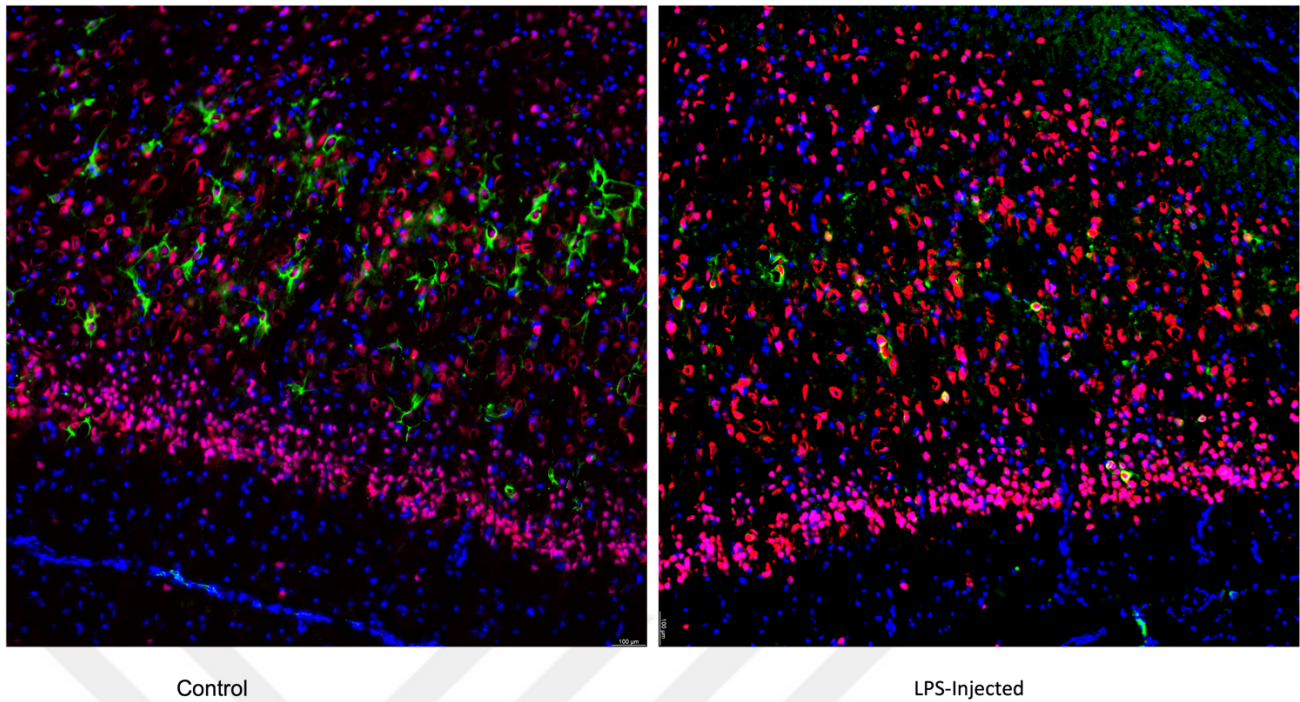


Figure 15 Loss of PNNs in LPS induced animals. On the left, IF stained brain slice of the PFC from a control animal (NeuN in red indicating neurons, WFA in green staining PNN structures and DAPI in blue). On the right: same staining applied on a brain slice of the PFC from an LPS-injected animal. Images depict a prominent loss of WFA+ neuronal surroundings in LPS-injected animals compared to controls.

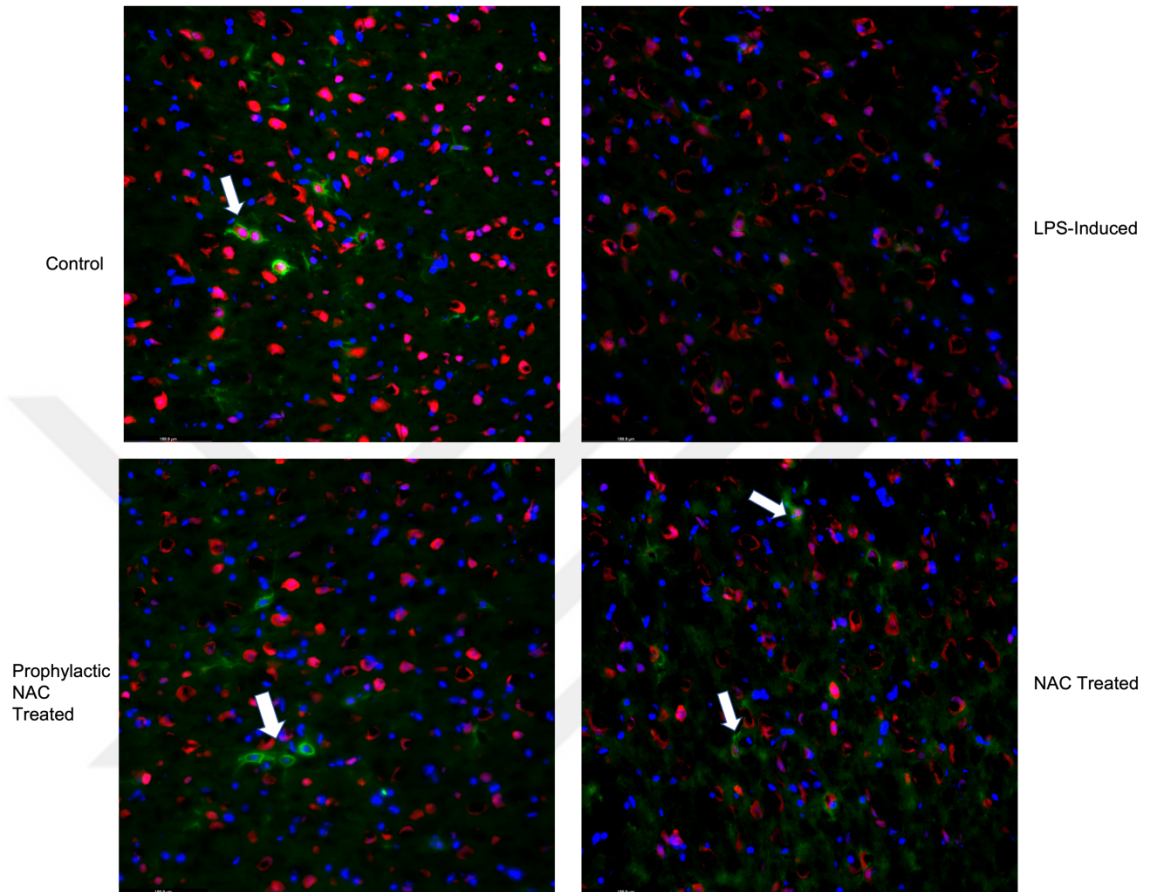


Figure 16 WFA stained PFCs in all groups. PNN surrounded neurons (white arrows). Red: NeuN, Blue: DAPI, Green: WFA. Staining against PNNs with WFA revealed a significant loss in PNN structures in regions of the PFC in LPS-induced animals. Stained brain slices from prophylactic NAC treated and NAC treated groups indicated that NAC provided some preservation of PNN structures against LPS.

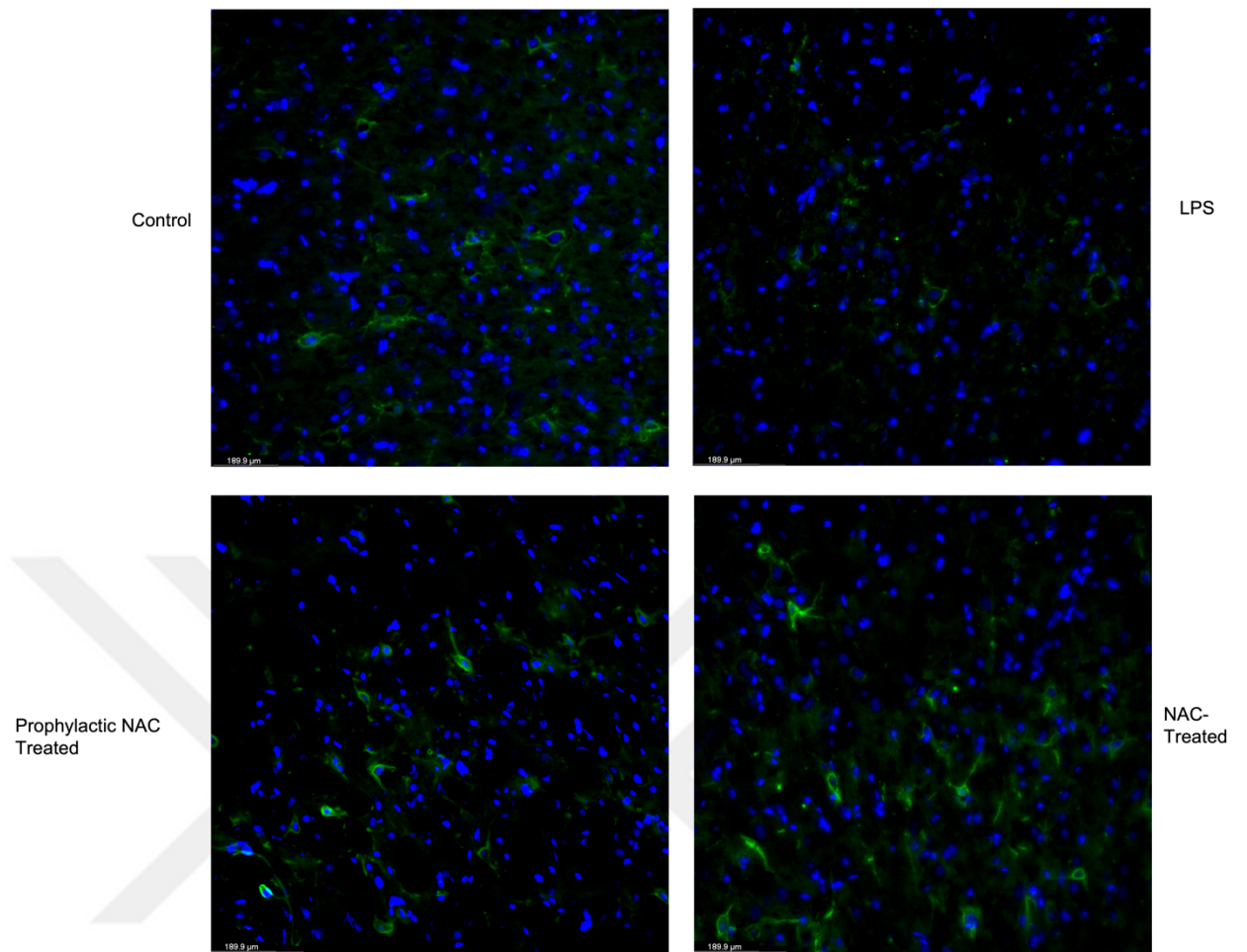


Figure 17 WFA stained PFCs in all groups. (Blue: DAPI, Green: WFA). Staining against PNNs with WFA revealed a significant loss in PNN structures in regions of the PFC in LPS-induced animals. Stained brain slices from prophylactic NAC treated and NAC treated groups indicated that NAC provided some preservation of PNN structures against LPS.

Chapter 4:

DISCUSSION

In this study, we aimed at demonstrating the neuroprotective role of NAC in an acute neuroinflammation model induced by intrahippocampal LPS in rats. Our goal was to assess the ability of NAC to attenuate LPS-induced components of neuroinflammation such as protein accumulation, neuronal loss and astrocytic activation. Moreover, we aimed at investigating whether LPS-induction in adult rat brain could lead to perineuronal net disruptions. It is important because it was long thought that these structures are almost impossible to reassemble after the closure of the critical period of plasticity, a structurally dynamic time window for perineuronal nets that allows the formation of new synapses. Upon the closure of the critical period, these specialized reticular structures provide a protective shield for neurons against environmental stressors like amyloid accumulations and oxidative stress components (Crasper et al, 2020), but it also limits the formation of new connections between neurons. Since our model was induced in adult rats, where perineuronal nets are shown to be fully mature and had lost their juvenile state-like plastic abilities, we wanted to assess the state of PNNs upon LPS-induced inflammation. Moreover, we wanted to investigate the ability of NAC to preserve PNN structures against inflammatory insult induced by LPS. Upon quantifying PNN surrounded neurons in the PFC of all groups, we found that intra-hippocampal LPS-injection caused a significant decrease in WFA+ neuronal surroundings, corresponding to loss in PNN structures. These results can be discussed with reference to findings presented by Crasper et al (2020), where they indicated that PNN loss in mouse models of AD is linked to microglial activation, and pharmacological depletion of microglia actually attenuated PNN loss. Moreover, their results demonstrate that degraded components of PNNs are found accumulated inside

dense core plaques (Crasper et al, 2020). Overall, rising evidence is clearly highlighting the importance of glial induced-ECM loss in models of neuroinflammation, as a bridge to understand neuronal vulnerability to oxidative damage and inflammatory insult. Furthermore, our results indicated that a single intra-hippocampal dose of LPS (10 µg) increased amyloid concentrations in brain and spinal cord homogenates when assessed with ELISA. These results align with previous literature demonstrating the impact of acute LPS-injection in inducing amyloidosis in rodents (Deng et al, 2014) (Batista CRA et al, 2019) (Wang et al, 2018) (Lee et al, 2008). However, Tau concentration measured by ELISA indicated a rising pattern detected in brain and spinal cord homogenates of LPS-injected animals but results did not reach significance. In their study, Wang et al (2018) showed that LPS given i.p at a dose of 10 mg/kg caused a significant increase in phosphorylated Tau when measured by immunoblotting on brain homogenates of Sprague Dawley rats 24h post administration, their results also indicated significantly high levels of Aβ 7 to 9 days post LPS injection but no correlation was made between both results. Previous literature indicates a probable causative role of Aβ accumulation in the formation of Tau tangles (Götz et al, 2001) (Lewis et al, 2001). However, no definitive conclusion has been made regarding the progressive impact of LPS in such models, especially that animal type and age, as well as route and duration of administration, all contribute to highly heterogeneous pathological phenotype (Batista et al, 2019) (Zakaria et al, 2017).

Assessed by Morris water maze 10 days after injection, animals in all experimental groups displayed a learning behaviour featured by reduced platform retention latency. However, when compared to controls, no significant difference in latency was seen in LPS-induced animals; which can be explained by the acute duration of our model (Zakaria et al, 2017) and that the resulting hippocampal neuronal loss seen in our LPS-induced group was not yet sufficient to cause memory dysfunction, whereas chronic-LPS injection was shown to cause spatial memory deficits (Wegrzyniak, 2018). These results align with findings indicated by (Bossu et al, 2019), where a single LPS injection in male Wistar rats caused no significant spatial memory loss tested by MWM 7 days post administration; our results also align with a study (Czerniawski, 2015) showing that acute LPS administration on rats does not affect MWM performance as it selectively disrupts other certain memory types. Different findings, however, were presented by Yamada et al, (1999), where a single intra-hippocampal LPS injection in

Wistar rats (5µg) resulted in spatial memory disturbance assessed by MWM 10 to 15 days post-administration. In a different study (Lee et al, 2008), rats injected intraperitoneally with (250 µg/kg) dose of LPS showed a worse performance in MWM test compared to controls.

In the present work, we demonstrated that LPS injected into the hippocampus caused significant neuronal loss evident by IF staining, these results align with previous literature (Yamada et al, 1999) (Lee et al, 2008). Astrocytes take up a percentage of about 1/3 of all cells in the CNS, occupying an important regulatory and immune function as well as providing trophic support to neurons. In cases of CNS insult, there is an upregulation in GFAP in astrocytes that indicates neurotoxic reactivity and transition to A1 phenotype and is mostly prominent close to injured brain regions (Giovannoni and Quintana, 2020). This phenotypic transition was shown to be associated with LPS-induced microglial activation (Liddelov et al, 2017). Thus, aligning with our expectations and previous literature (Fu *et al.* 2014) (Houdek et al, 2014), LPS-injection also produced significant astrogliosis indicated by elevated GFAP staining in hippocampal regions. Astrocytic activation in LPS-treated adult rat hippocampus is believed to play a role in clearing neuronal apoptotic debris (Cerbai et al, 2012). However, it is still not clear whether this reactivity is responsible for initiating the vicious cycle of neuronal damage or is solely a protective reaction to halt to progression of damage.

NAC is a natural compound with evident anti-oxidant and anti-inflammatory impact acting as a scavenger for ROS and regulating the release of critical inflammatory cytokines (Mokhtari et al, 2017). Having no recorded side effects (Tardiolo et al, 2018) it has attracted the interest of medical researchers for decades, and raised hope for its potential therapeutic applications in neurodegenerative and neuropsychiatric disorders. In our model, we used NAC by giving it intraperitoneally to LPS-injected rats. As we further wanted to test potential prophylaxis impact, we incorporated an additional experimental group in which animals received an i.p dose of NAC (200 mg/kg) prior to model induction as well as further treatment doses. Our results indicated that prophylactic NAC treatment prevented LPS-induced neuronal loss, however, direct treatment administration did not show significant neuronal protection when compared to LPS-injected group. These findings indicate a potential neuro-protective impact of prophylactic NAC use against acute neuroinflammatory cellular loss, and align with

previous evidence on its anti-apoptotic abilities through reducing damage associated NF- κ B and TNF secretions (Shahripour et al, 2014) as well as in aging and neurodegenerative inflammation (Chandra et al, 2000). Another study conducted by Fu et al (2006), highlighted that pretreatment with NAC (i.p. 200 mg/kg) significantly preserved neuronal count as well as learning and memory in A β -treated mice. Additionally, NAC treatment (prophylactic and post-LPS injection) kept A β concentration in brain and spinal cord samples close to controls while it significantly elevated by LPS-induction; interestingly, in their study (Joy et al, 2019) showed that i.p. administration of NAC a week before and a week after ICV colchicine could not reduce amyloid pathology. On the other hand, NAC was able to reduce astrogliosis in their model which is what we also demonstrated in the present study; Both pre-treated and post-LPS injection NAC treated groups indicated a prominently significant reduction in brain astrogliosis when compared to LPS-injected groups.

Furthermore, our present work highlights the potential role of NAC in rescuing and maintaining PNN loss associated with inflammatory damage. Our results clearly indicate that NAC treated groups had more intact PNN structures and higher number of WFA+ stained perineuronal areas when compared to LPS-induced groups.

Indeed, these findings are important because PNNs serve as the initial protective barrier for neurons against inflammatory and oxidative stress insult. If this natural compound could preserve the integrity of PNN structural deformation, it could hold an important neuro-protective potential against acute inflammatory damage, and opens up a new path in the field of neurodegeneration research focusing on the role of ECM and neuronal vulnerability in certain pathological conditions.

Chapter 5

CONCLUSION

To conclude, as variable and heterogenous, models of neuroinflammation could bring us closer to deciphering important molecular pathways and help us understand the order of pathological processes involved in neurodegeneration. Also, understanding what happens in acute states holds promise for possible early intervention. Furthermore, neuron-extracellular matrix interactions play an essential role in several neurodegenerative diseases, thus, understanding the basic mechanisms underlying this phenomenon helps in guiding towards better and more efficient treatments.

PNNs have only recently attracted focus and we still lack a significant knowledge of their structures and ways of action in oxidative stress related pathology and synaptic plasticity.

This present study provides a step towards understanding the link between neurodegeneration and perineuronal net disruptions, and highlights the potential of NAC in preventing early inflammatory insult.

Bibliography

1. Jeong HK, Ji K, Min K, Joe EH. Brain inflammation and microglia: facts and misconceptions. *Exp Neurobiol*. 2013 Jun;22(2):59-67. doi: 10.5607/en.2013.22.2.59. Epub 2013 Jun 27. PMID: 23833554; PMCID: PMC3699675.
2. Wang, S., & Qi, X. (2022). The Putative Role of Astaxanthin in Neuroinflammation Modulation: Mechanisms and Therapeutic Potential. *Frontiers in Pharmacology*, 13. <https://doi.org/10.3389/fphar.2022.916653>
3. Nazem, A., Sankowski, R., Bacher, M., & Al-Abed, Y. (2015). Rodent models of neuroinflammation for Alzheimer's disease. *Journal of Neuroinflammation*, 12(1), 74. <https://doi.org/10.1186/s12974-015-0291-y>
4. Troncoso-Escudero, P., Parra, A., Nassif, M., & Vidal, R. L. (2018). Outside in: Unraveling the Role of Neuroinflammation in the Progression of Parkinson's Disease. *Frontiers in Neurology*, 9. <https://doi.org/10.3389/fneur.2018.00860>
5. Bjelobaba, I., Savic, D., & Lavrnja, I. (2017). Multiple Sclerosis and Neuroinflammation: The Overview of Current and Prospective Therapies. *Current Pharmaceutical Design*, 23(5), 693–730. <https://doi.org/10.2174/1381612822666161214153108>
6. More, S. V., Kumar, H., Kim, I. S., Song, S.-Y., & Choi, D.-K. (2013). Cellular and molecular mediators of neuroinflammation in the pathogenesis of Parkinson's disease. *Mediators of Inflammation*, 2013, 952375. <https://doi.org/10.1155/2013/952375>
7. Anwar, M. M. (2022). Oxidative stress-A direct bridge to central nervous system homeostatic dysfunction and Alzheimer's disease. In *Cell Biochemistry and Function* (Vol. 40, Issue 1, pp. 17–27). John Wiley and Sons Ltd. <https://doi.org/10.1002/cbf.3673>
8. Sayre, L., Smith, M., & Perry, G. (2001). Chemistry and Biochemistry of Oxidative Stress in Neurodegenerative Disease. *Current Medicinal Chemistry*, 8(7), 721–738. <https://doi.org/10.2174/0929867013372922>
9. Birecree, E., Whetsell, W. O., Stoscheck, C., King, L. E., & Nanney, L. B. (1988). Immunoreactive Epidermal Growth Factor Receptors in Neuritic

Plaques from Patients with Alzheimer's Disease. *Journal of Neuropathology & Experimental Neurology*, 47(5), 549–560. <https://doi.org/10.1097/00005072-198809000-00006>

10. Amor S, Puentes F, Baker D, van der Valk P. Inflammation in neurodegenerative diseases. *Immunology*. 2010 Feb;129(2):154-69. doi: 10.1111/j.1365-2567.2009.03225.x. PMID: 20561356; PMCID: PMC2814458.
11. Sugaya K, Chou S, Xu SJ, McKinney M. Indicators of glial activation and brain oxidative stress after intraventricular infusion of endotoxin. *Brain Res Mol Brain Res*. 1998 Jul 15;58(1-2):1-9. doi: 10.1016/s0169-328x(97)00365-3. PMID: 9685567
12. Lee, J.W., Lee, Y.K., Yuk, D.Y. *et al.* Neuro-inflammation induced by lipopolysaccharide causes cognitive impairment through enhancement of beta-amyloid generation. *J Neuroinflammation* 5, 37 (2008). <https://doi.org/10.1186/1742-2094-5-37>
13. Batista CRA, Gomes GF, Candelario-Jalil E, Fiebich BL, de Oliveira ACP. Lipopolysaccharide-Induced Neuroinflammation as a Bridge to Understand Neurodegeneration. *Int J Mol Sci*. 2019 May 9;20(9):2293. doi: 10.3390/ijms20092293. PMID: 31075861; PMCID: PMC6539529
14. Zhao, J., Bi, W., Xiao, S. *et al.* Neuroinflammation induced by lipopolysaccharide causes cognitive impairment in mice. *Sci Rep* 9, 5790 (2019). <https://doi.org/10.1038/s41598-019-42286-8>
15. Koedel U, Merbt UM, Schmidt C, Angele B, Popp B, Wagner H, Pfister HW, Kirschning CJ. Acute brain injury triggers MyD88-dependent, TLR2/4-independent inflammatory responses. *Am J Pathol*. 2007 Jul;171(1):200-13. doi: 10.2353/ajpath.2007.060821. PMID: 17591966; PMCID: PMC1941591
16. Amor S, Puentes F, Baker D, van der Valk P. Inflammation in neurodegenerative diseases. *Immunology*. 2010 Feb;129(2):154-69. doi: 10.1111/j.1365-2567.2009.03225.x. PMID: 20561356; PMCID: PMC2814458
17. Arvanitakis Z, Shah RC, Bennett DA. Diagnosis and Management of Dementia: Review. *JAMA*. 2019 Oct 22;322(16):1589-1599. doi: 10.1001/jama.2019.4782. PMID: 31638686; PMCID: PMC7462122.
18. Hebert LE, Weuve J, Scherr PA, Evans DA. Alzheimer disease in the United States (2010-2050) estimated using the 2010 census. *Neurology*. 2013 May

7;80(19):1778-83. doi: 10.1212/WNL.0b013e31828726f5. Epub 2013 Feb 6. PMID: 23390181; PMCID: PMC3719424.

19. Pal, K., Mukadam, N., Petersen, I. et al. Mild cognitive impairment and progression to dementia in people with diabetes, prediabetes and metabolic syndrome: a systematic review and meta-analysis. *Soc Psychiatry Psychiatr Epidemiol* 53, 1149–1160 (2018). <https://doi.org/10.1007/s00127-018-1581-3>
20. Gupta A, Preis SR, Beiser A, Devine S, Hanke L, Seshadri S, Wolf PA, Au R. Mid-life Cardiovascular Risk Impacts Memory Function: The Framingham Offspring Study. *Alzheimer Dis Assoc Disord*. 2015 Apr-Jun;29(2):117-23. doi: 10.1097/WAD.000000000000059. PMID: 25187219; PMCID: PMC4345145
21. LoBue C, Munro C, Schaffert J, Didehbani N, Hart J, Batjer H, Cullum CM. Traumatic Brain Injury and Risk of Long-Term Brain Changes, Accumulation of Pathological Markers, and Developing Dementia: A Review. *J Alzheimers Dis*. 2019;70(3):629-654. doi: 10.3233/JAD-190028. PMID: 31282414
22. Ahmad MA, Kareem O, Khushtar M, Akbar M, Haque MR, Iqbal A, Haider MF, Pottoo FH, Abdulla FS, Al-Haidar MB, Alhajri N. Neuroinflammation: A Potential Risk for Dementia. *Int J Mol Sci*. 2022 Jan 6;23(2):616. doi: 10.3390/ijms23020616. PMID: 35054805; PMCID: PMC8775769.
23. Qiu C, Kivipelto M, von Strauss E. Epidemiology of Alzheimer's disease: occurrence, determinants, and strategies toward intervention. *Dialogues Clin Neurosci*. 2009;11(2):111-28. doi: 10.31887/DCNS.2009.11.2/cqiu. PMID: 19585947; PMCID: PMC3181909
24. Hurd MD, Martorell P, Delavande A, Mullen KJ, Langa KM. Monetary costs of dementia in the United States. *N Engl J Med*. 2013 Apr 4;368(14):1326-34. doi: 10.1056/NEJMsa1204629. PMID: 23550670; PMCID: PMC3959992
25. Katafuchi T, Ifuku M, Mawatari S, Noda M, Miake K, Sugiyama M, Fujino T. Effects of plasmalogens on systemic lipopolysaccharide-induced glial activation and β -amyloid accumulation in adult mice. *Ann N Y Acad Sci*. 2012 Jul;1262:85-92. doi: 10.1111/j.1749-6632.2012.06641.x. PMID: 22823439
26. Krstic, D., Madhusudan, A., Doehner, J. et al. Systemic immune challenges trigger and drive Alzheimer-like neuropathology in mice. *J Neuroinflammation* 9, 151 (2012). <https://doi.org/10.1186/1742-2094-9-151>
27. Amin AF, Shaaban OM, Bediawy MA. N-acetyl cysteine for treatment of recurrent unexplained pregnancy loss. *Reprod Biomed Online*. 2008

- Nov;17(5):722-6. doi: 10.1016/s1472-6483(10)60322-7. PMID: 18983759.
28. Moreira PI, Harris PL, Zhu X, Santos MS, Oliveira CR, Smith MA, Perry G. Lipoic acid and N-acetyl cysteine decrease mitochondrial-related oxidative stress in Alzheimer disease patient fibroblasts. *J Alzheimers Dis.* 2007 Sep;12(2):195-206. doi: 10.3233/jad-2007-12210. PMID: 17917164
29. Mokhtari V, Afsharian P, Shahhoseini M, Kalantar SM, Moini A. A Review on Various Uses of N-Acetyl Cysteine. *Cell J.* 2017 Apr-Jun;19(1):11-17. doi: 10.22074/cellj.2016.4872. Epub 2016 Dec 21. PMID: 28367412; PMCID: PMC5241507
30. Fu AL, Dong ZH, Sun MJ. Protective effect of N-acetyl-L-cysteine on amyloid beta-peptide-induced learning and memory deficits in mice. *Brain Res.* 2006 Sep 13;1109(1):201-6. doi: 10.1016/j.brainres.2006.06.042. Epub 2006 Jul 26. PMID: 16872586.
31. Bavarsad Shahripour R, Harrigan MR, Alexandrov AV. N-acetylcysteine (NAC) in neurological disorders: mechanisms of action and therapeutic opportunities. *Brain Behav.* 2014 Mar;4(2):108-22. doi: 10.1002/brb3.208. Epub 2014 Jan 13. PMID: 24683506; PMCID: PMC3967529
32. Aruoma OI, Halliwell B, Hoey BM, Butler J. The antioxidant action of N-acetylcysteine: its reaction with hydrogen peroxide, hydroxyl radical, superoxide, and hypochlorous acid. *Free Radic Biol Med.* 1989;6(6):593-7. doi: 10.1016/0891-5849(89)90066-x. PMID: 2546864
33. H.Wen T, K.Binder D, M.Ethell I, A.Razak K, The Perineuronal 'Safety' Net? Perineuronal Net Abnormalities in Neurological Disorders, *Front. Mol. Neurosci.*, 03 August 2018, <https://doi.org/10.3389/fnmol.2018.00270>.
34. Reichelt AC, Hare DJ, Bussey TJ, Saksida LM. Perineuronal Nets: Plasticity, Protection, and Therapeutic Potential. *Trends Neurosci.* 2019 Jul;42(7):458-470. doi: 10.1016/j.tins.2019.04.003. Epub 2019 Jun 4. PMID: 31174916
35. Pizzorusso T, Medini P, Berardi N, Chierzi S, Fawcett JW, Maffei L. Reactivation of ocular dominance plasticity in the adult visual cortex. *Science.* 2002 Nov 8;298(5596):1248-51. doi: 10.1126/science.1072699. PMID: 12424383

36. Jakovljević A, Tucić M, Blažiková M, Korenić A, Missirlis Y, Stamenković V, Andjus P. Structural and Functional Modulation of Perineuronal Nets: In Search of Important Players with Highlight on Tenascins. *Cells*. 2021 May 29;10(6):1345. doi: 10.3390/cells10061345. PMID: 34072323; PMCID: PMC8230358
37. Suttkus A, Holzer M, Morawski M, Arendt T. The neuronal extracellular matrix restricts distribution and internalization of aggregated Tau-protein. *Neuroscience*. 2016 Jan 28;313:225-35. doi: 10.1016/j.neuroscience.2015.11.040. Epub 2015 Nov 24. PMID: 26621125
38. Mauney SA, Athanas KM, Pantazopoulos H, Shaskan N, Passeri E, Berretta S, Woo TU. Developmental pattern of perineuronal nets in the human prefrontal cortex and their deficit in schizophrenia. *Biol Psychiatry*. 2013 Sep 15;74(6):427-35. doi: 10.1016/j.biopsych.2013.05.007. Epub 2013 Jun 19. PMID: 23790226; PMCID: PMC3752333
39. Reichelt AC. Is loss of perineuronal nets a critical pathological event in Alzheimer's disease? *EBioMedicine*. 2020 Sep, 59:102946. doi: 10.1016/j.ebiom.2020.102946. Epub 2020 Aug 15. PMID: 32810826; PMCID: PMC7452426
40. Crapser JD, Spangenberg EE, Barahona RA, Arreola MA, Hohsfield LA, Green KN. Microglia facilitate loss of perineuronal nets in the Alzheimer's disease brain. *EBioMedicine*. 2020 Aug;58:102919. doi: 10.1016/j.ebiom.2020.102919. Epub 2020 Jul 31. PMID: 32745992; PMCID: PMC7399129
41. Sharmin S, Pradhan J, Zhang Z, Bellingham M, Simmons D, Piper M. Perineuronal net abnormalities in *Slc13a4*^{+/-} mice are rescued by postnatal administration of N-acetylcysteine. *Exp Neurol*. 2021 Aug;342:113734. doi: 10.1016/j.expneurol.2021.113734. Epub 2021 May 1. PMID: 33945789.
42. Cabungcal JH, Steullet P, Kraftsik R, Cuenod M, Do KQ. Early-life insults impair parvalbumin interneurons via oxidative stress: reversal by N-acetylcysteine. *Biol Psychiatry*. 2013 Mar 15;73(6):574-82. doi: 10.1016/j.biopsych.2012.09.020. Epub 2012 Nov 7. PMID: 23140664.
43. Espinosa-Oliva, A. M., de Pablos, R. M., & Herrera, A. J. (2013). *Intracranial Injection of LPS in Rat as Animal Model of Neuroinflammation* (pp. 295–305). https://doi.org/10.1007/978-1-62703-520-0_26

44. Morris, R., Garrud, P., Rawlins, J. *et al.* Place navigation impaired in rats with hippocampal lesions. *Nature* **297**, 681–683 (1982)
<https://doi.org/10.1038/297681a0>
45. Shahidi S, Zargooshnia S, Asl SS, Komaki A, Sarihi A. Influence of N-acetyl cysteine on beta-amyloid-induced Alzheimer's disease in a rat model: A behavioral and electrophysiological study. *Brain Res Bull.* 2017 May;131:142-149. doi: 10.1016/j.brainresbull.2017.04.001. Epub 2017 Apr 11. PMID: 28411131.
46. Joy, T., Rao, M. S., Madhyastha, S., & Pai, K. (2019). Effect of N-Acetyl Cysteine on Intracerebroventricular Colchicine Induced Cognitive Deficits, Beta Amyloid Pathology, and Glial Cells. *Neuroscience Journal*, 2019, 1–15.
<https://doi.org/10.1155/2019/7547382>
47. Catorce MN, Gevorkian G. LPS-induced Murine Neuroinflammation Model: Main Features and Suitability for Pre-clinical Assessment of Nutraceuticals. *Curr Neuropharmacol.* 2016;14(2):155-64. doi: 10.2174/1570159x14666151204122017. PMID: 26639457; PMCID: PMC4825946
48. Deng X, Li M, Ai W, He L, Lu D, Patrylo PR, Cai H, Luo X, Li Z, Yan X. Lipopolysaccharide-Induced Neuroinflammation Is Associated with Alzheimer-Like Amyloidogenic Axonal Pathology and Dendritic Degeneration in Rats. *Adv Alzheimer Dis.* 2014 Jun;3(2):78-93. doi: 10.4236/aad.2014.32009. PMID: 25360394; PMCID: PMC4211261
49. Hauss-Wegrzyniak B, Dobrzanski P, Stoehr JD, Wenk GL. Chronic neuroinflammation in rats reproduces components of the neurobiology of Alzheimer's disease. *Brain Res.* 1998 Jan 12;780(2):294-303. doi: 10.1016/s0006-8993(97)01215-8. PMID: 9507169.
50. Wang LM, Wu Q, Kirk RA, Horn KP, Ebada Salem AH, Hoffman JM, Yap JT, Sonnen JA, Towner RA, Bozza FA, Rodrigues RS, Morton KA. Lipopolysaccharide endotoxemia induces amyloid- β and p-tau formation in the rat brain. *Am J Nucl Med Mol Imaging.* 2018 Apr 25;8(2):86-99. PMID: 29755842; PMCID: PMC5944824
51. Götz J, Chen F, van Dorpe J, Nitsch RM. Formation of neurofibrillary tangles in P3011 tau transgenic mice induced by A β 42 fibrils. *Science.* 2001 Aug 24;293(5534):1491-5. doi: 10.1126/science.1062097. PMID: 11520988

52. Lewis J, Dickson DW, Lin WL, Chisholm L, Corral A, Jones G, Yen SH, Sahara N, Skipper L, Yager D, Eckman C, Hardy J, Hutton M, McGowan E. Enhanced neurofibrillary degeneration in transgenic mice expressing mutant tau and APP. *Science*. 2001 Aug 24;293(5534):1487-91. doi: 10.1126/science.1058189. PMID: 11520987
53. Zakaria R, Wan Yaacob WM, Othman Z, Long I, Ahmad AH, Al-Rahbi B. Lipopolysaccharide-induced memory impairment in rats: a model of Alzheimer's disease. *Physiol Res*. 2017 Sep 22;66(4):553-565. doi: 10.33549/physiolres.933480. Epub 2017 Apr 12. PMID: 28406691.
54. K Yamada, Y Komori, T Tanaka, K Senzaki, T Nikai, H Sugihara, T Kameyama, T Nabeshima, Brain dysfunction associated with an induction of nitric oxide synthase following an intracerebral injection of lipopolysaccharide in rats, *Neuroscience*, Volume 88, Issue 1, 1999, Pages 281-294, ISSN 0306-4522, [https://doi.org/10.1016/S0306-4522\(98\)00237-1](https://doi.org/10.1016/S0306-4522(98)00237-1).
55. Bossù P, Cutuli D, Palladino I, Caporali P, Angelucci F, Laricchiuta D, Gelfo F, De Bartolo P, Caltagirone C, Petrosini L. A single intraperitoneal injection of endotoxin in rats induces long-lasting modifications in behavior and brain protein levels of TNF- α and IL-18. *J Neuroinflammation*. 2012 May 29;9:101. doi: 10.1186/1742-2094-9-101. PMID: 22642744; PMCID: PMC3444884
56. Czerniawski J, Miyashita T, Lewandowski G, Guzowski JF. Systemic lipopolysaccharide administration impairs retrieval of context-object discrimination, but not spatial, memory: Evidence for selective disruption of specific hippocampus-dependent memory functions during acute neuroinflammation. *Brain Behav Immun*. 2015 Feb; 44:159-66. doi: 10.1016/j.bbi.2014.09.014. Epub 2014 Oct 19. PMID: 25451612; PMCID: PMC4358899
57. zHoudek HM, Larson J, Watt JA, Rosenberger TA. Bacterial lipopolysaccharide induces a dose-dependent activation of neuroglia and loss of basal forebrain cholinergic cells in the rat brain. *Inflamm Cell Signal*. 2014;1(1):e47. doi: 10.14800/ics.47. PMID: 26052539; PMCID: PMC4457330
58. Fu HQ, Yang T, Xiao W, Fan L, Wu Y, Terrando N, Wang TL. Prolonged neuroinflammation after lipopolysaccharide exposure in aged rats. *PLoS One*.

2014 Aug 29;9(8):e106331. doi: 10.1371/journal.pone.0106331. PMID: 25170959; PMCID: PMC4149545

59. David JP, Ghozali F, Fallet-Bianco C, Watzet A, Delaine S, Boniface B, Di Menza C, Delacourte A. Glial reaction in the hippocampal formation is highly correlated with aging in human brain. *Neurosci Lett*. 1997 Oct 10;235(1-2):53-6. doi: 10.1016/s0304-3940(97)00708-8. PMID: 9389594
60. Mokhtari V, Afsharian P, Shahhoseini M, Kalantar SM, Moini A. A Review on Various Uses of N-Acetyl Cysteine. *Cell J*. 2017 Apr-Jun;19(1):11-17. doi: 10.22074/cellj.2016.4872. Epub 2016 Dec 21. PMID: 28367412; PMCID: PMC5241507
61. Crapser JD, Spangenberg EE, Barahona RA, Arreola MA, Hohsfield LA, Green KN. Microglia facilitate loss of perineuronal nets in the Alzheimer's disease brain. *EBioMedicine*. 2020 Aug;58:102919. doi: 10.1016/j.ebiom.2020.102919. Epub 2020 Jul 31. PMID: 32745992; PMCID: PMC7399129
62. Tardiolo G, Bramanti P, Mazzon E. Overview on the Effects of N-Acetylcysteine in Neurodegenerative Diseases. *Molecules*. 2018 Dec 13;23(12):3305. doi: 10.3390/molecules23123305. PMID: 30551603; PMCID: PMC6320789
63. Chandra J, Samali A, Orrenius S. Triggering and modulation of apoptosis by oxidative stress. *Free Radic Biol Med*. 2000 Aug;29(3-4):323-33. doi: 10.1016/s0891-5849(00)00302-6. PMID: 11035261
64. Joy T, Rao MS, Madhyastha S, Pai K. Effect of N-Acetyl Cysteine on Intracerebroventricular Colchicine Induced Cognitive Deficits, Beta Amyloid Pathology, and Glial Cells. *Neurosci J*. 2019 Apr 15;2019:7547382. doi: 10.1155/2019/7547382. PMID: 31139638; PMCID: PMC6500609
65. Giovannoni F, Quintana FJ. The Role of Astrocytes in CNS Inflammation. *Trends Immunol*. 2020 Sep;41(9):805-819. doi: 10.1016/j.it.2020.07.007. Epub 2020 Aug 13. PMID: 32800705; PMCID: PMC8284746
66. Liddelov, S., Guttenplan, K., Clarke, L. *et al*. Neurotoxic reactive astrocytes are induced by activated microglia. *Nature* **541**, 481–487 (2017). <https://doi.org/10.1038/nature21029>

